JEOFİZİK 4, 3-35, 1990

QUATERNARY TECTONIC AND SEDIMENTARY HISTORY OF EASTERN AEGEAN SEA SHELF AREA

Doğu Ege Denizi Şelf Alanının Kuvaterner'deki Tektoniği ve Tortul Tarihçesi

A.E. AKSU*, T. KONUK** , A. ULUĞ**, M. DUMAN** and D.J.W. PIPER+

ABSTRACT

Air-gun and 3.5-kHz seismic profiles from the eastern Aegean Sea show that the continental shelf off major rivers is formed by several superimposed deltaic sequences. The present-day shelf break denotes the topset to foreset transition of the latest Pleistocene delta. Micropaleontological and stable isotopic data in cores from the shelf break area indicate that these sediments were deposited when the sea level was about 100-110 m below its present position in a brackish water environment. There are at least two older shelf breaks at depth that probably represent earlier delta progradation during glacially lowered sea-level settings. During times of lowered and gradually fluctuating sea level associated with late Quaternary glaciations, deltas prograded seaward 40-60 km from their present positions. Foreset progradation ceased with the postglacial sea level rise and deltas were re-established far inland in drowned river valleys. Between the present coastline and the shelf break several lenticular seismic units are found shingled one on top another; they are interpreted as transgressive deltaic and marine deposits. The coastal shelf and basins are subsiding at an average rate of about 1 m per 1000 years. This tectonic subsidence, which is probably accentuated by the loading effects of the deltas, manifests itself as widespread normal block faulting which can be related to the pre-Miocene structural framework of the region. In addition to deformation related to this faulting and associated fluid venting, synsedimentary deformation structures occur in places immediately seaward of prograded delta foresets.

ÖZET

Doğu Ege Denizi'nden alınan hava tabancası ve 3.5 kHz sismik kayıtları büyük nehirlerin açığındaki kıta sahanlığının, birbirinin üzerine binmiş deltalardan oluştuğunu göstermektedir. Güncel kıta sınırı, Geç Pleyistosen deltasının, delta düzlüğünden delta önüne (topset to foreset) geçişini belirtmektedir. Bu kıta sınırı bölgesinden alınan karotlardaki mikropaleontolojik ve duraylı izotop verileri, bu sedimentlerin denizlerin bu günkü deniz seviyesinden yaklaşık 100-110 m altında olduğu zamanki bölgelerde çökeldiğini göstermektedir. Burada deniz tabanından daha derinde, daha önceki buzul dönemlerinin alçak deniz seviyelerinde gelişmiş delta ilerlemelerini simgeleyen en az iki adet Pleyistosen yaşlı kıta sınırı görülmektedir. Kuvaterner'deki son buzullanma ile ilgili alçak deniz seviyelerinde (veya deniz seviyesinin alçalırken gösterdiği değişimler sırasında), deltalar güncel kıyı şeridinden 40 ile 60 km denize doğru ilerleme göstermişlerdir. Buzul devri sonunda deniz seviyesindeki yükselmelerle beraber deltalarda, delta önü ilerlemesi durmuş ve bunlar transgresyonun en son safhasında yeniden karalardaki eski nehir vadilerine yerleşmişlerdir. Güncel kıyı şeridi ile kıta sınırı (70 m eşderinlik çizgisi) arasında muhtelif merceksel sismik birimlerin birbirleri üzerine kiremitler gibi yerleştikleri görülmüş ve bunların transgresif delta ve deniz çökelleri olarak değerlendirilmesi yapılmıştır. Kıyıya yakın sahanlığın ve havzaların 1000 yılda yaklaşık 1 m gibi bir tektonik çökme gösterdiği saptanmıştır. Muhtemelen deltaların yüklenmesi ile belirtilen bu tektonik çökme, bölgenin Miyosen öncesi yapısal durumu ile ilgili olan ve geniş bölgeler kapsayan normal faylanmalar şeklinde kendini gösterir. Faylanmaya ve sıvı kaçışına bağlı deformasyon dışında özellikle delta önü tabakalarında çeşitli eş zamanlı deformasyonlar da görülmüştür.

* Department of Earth Sciences, Memorial University of Newfoundland, St. John's, Newfoundland, Canada, AlB 3X5

** Institute of Marine Sciences and Technology, Dokuz Eylül University, SSK Blok D, Kat 2, Konak, Izmir.

\+ Atlantic Geoscience Centre, Geological Survey of Canada, Bedford Institute of Oceanography, Box 1006, Dartmouth, Nova Scotia, Canada, B2Y 4A2

INTRODUCTION

The neotectonic framework of western Turkey is characterized by numerous east-west trending grabens, associated with the regional north-south extension of the Aegean plate

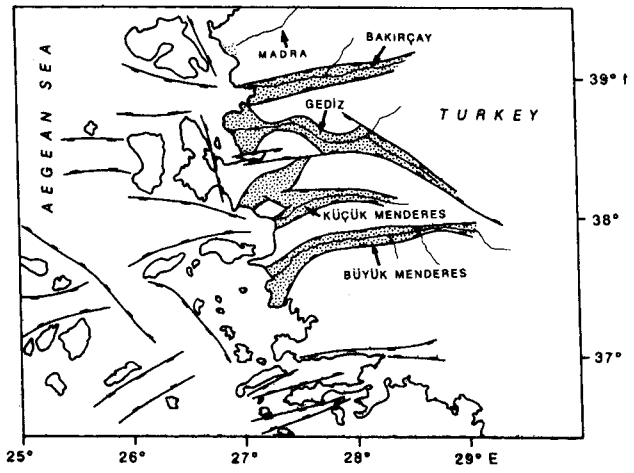

Fig. 1. Tectonic framework of the eastern Aegean Sea. Data from Arpat and Şaroğlu (1975), Dewey and Şengör (1979), Angelier *et al.* (1981) and Galanopoulos and Delibasis (1971). Stippled areas refer to Neogene and Quaternary deposits in grabens. Gediz, Bakırçay and Madra deltas are shown in Fig. 2; Büyük and Küçük Menderes deltas are shown in Figs. 3 and 4, respectively.

Şekil 1. Doğu Ege Denizi'nin tektonik yerleşimi. Veriler Arpat ve Şaroğlu (1975), Dewey ve Şengör (1979), Angelier ve diğ. (1981), ve Galanopoulas ve Delibasis (1971)'den alınmıştır. Noktalı alanlar grabenlerdeki Neojen ve Kuvaterner çökellerini göstermektedir. Gediz, Bakırçay ve Madra deltaları Şekil 2'de, Büyük ve Küçük Menderes deltaları da Şekil 3 ve Şekil 4'de gösterilmiştir.

(Fig. 1; Arpat and Şaroğlu 1975, Dewey and Şengör 1979, Angelier *et al.* 1981). These grabens and the intervening horsts control the west flowing drainage systems of western Turkey. Seismic studies have shown similar graben systems in the eastern Aegean Sea, which are presumably correlated with their **subaerial** counterparts (Galanapoulos and Delibasis 1971). Few investigations have been carried out on the sedimentary and tectonic histories of the continental shelves surrounding the Aegean Sea (Flemming 1972, Venkatarathnam *et al.* 1972, Lykousis *et al.* 1981, Aksu and Piper 1983, Aksu *et al.* 1987a, 1987b).

In this paper, we examine the late Quaternary growth of the Gediz, Bakırçay, Madra, Büyük Menderes and Küçük Menderes deltas at basin margins in the eastern Aegean Sea. The Gediz and Bakırçay are river-dominated deltas, whereas Madra, Büyük Menderes and Küçük Menderes are wave-dominated deltas. They were built in small grabens of a back-arc setting in the Mediterranean Sea during the fluctuating sea-level of the Quaternary. These deltas are relatively small, so that the seismic stratigraphy of a complete progressive and regressive cycle and the vertical and lateral sedimentary facies relationships can be studied in detail using high-resolution seismic profiles and cores. Therefore, they may serve as modern analogues of the ancient deltaic sequences developed in shallow epicontinental sea-ways.

STUDY AREA

The study area extends from 37°25'N to 39°15'N and 26°25'E to 27°00'E and includes the Izmir, Çandarlı and Dikili Bays (Fig. 2) and the Gulfs of Kuşadası and Güllük (Figs. 3,4). The Gediz river drains into Izmir Bay and in the late Pleistocene its delta prograded northwards into the 350 m deep Karaburun Basin, south of the island of Lesbos. The pre-

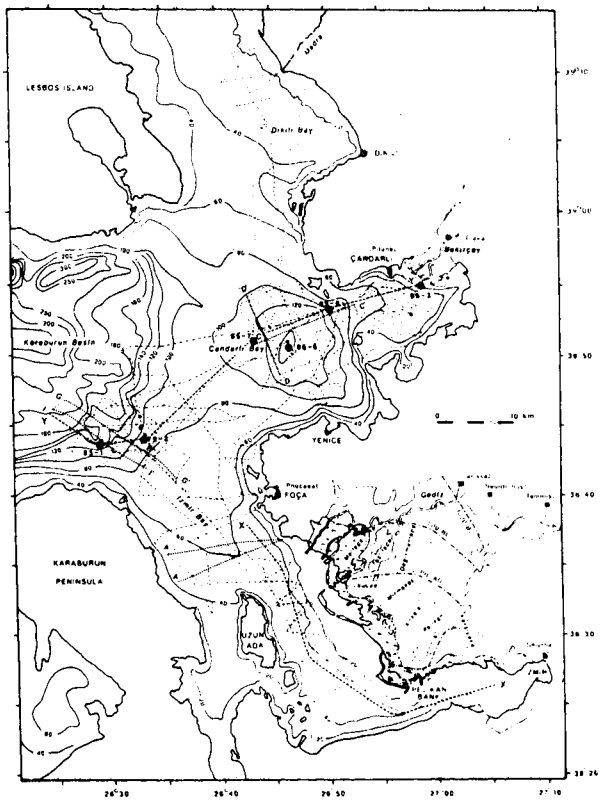

Fig. 2. Bathymetric map of Izmir Bay and Çandarlı Bay, showing seismic profiles, cores (solid circles), present rivers, abandoned channels, the position of former shorelines and classical Greek and Roman cities (in parentheses). Isobaths are in metres A-A', C-C, D-D', G-G' and I-I', are seismic sections illustrated in Figs. 6, 8, 9, 15 and 30, respectively. X-X' and Y-Y' are schematic geological cross-sections illustrated in Figs. 14 and 25.

Şekil 2. Sismik profilleri , karot alım yerlerini (içi dolu daireler), güncel nehirler, terkedilmiş kanallar, eski kıyı hatlarını ve Eski Latin şehirlerini (parantezler içerisinde) gösteren İzmir ve Çandarlı Körfezi Batimetri Haritası. Derinlikler metre olup, A-A', C-C', D-D', G-G' ve I-I' Şekil 6, 8, 9, 15 ve 30'da verilen sismik profilleri, X-X' ve Y-Y' ise Şekil 14 ve 28'de verilen şematik jeolojik kesitleri belirtmektedir.

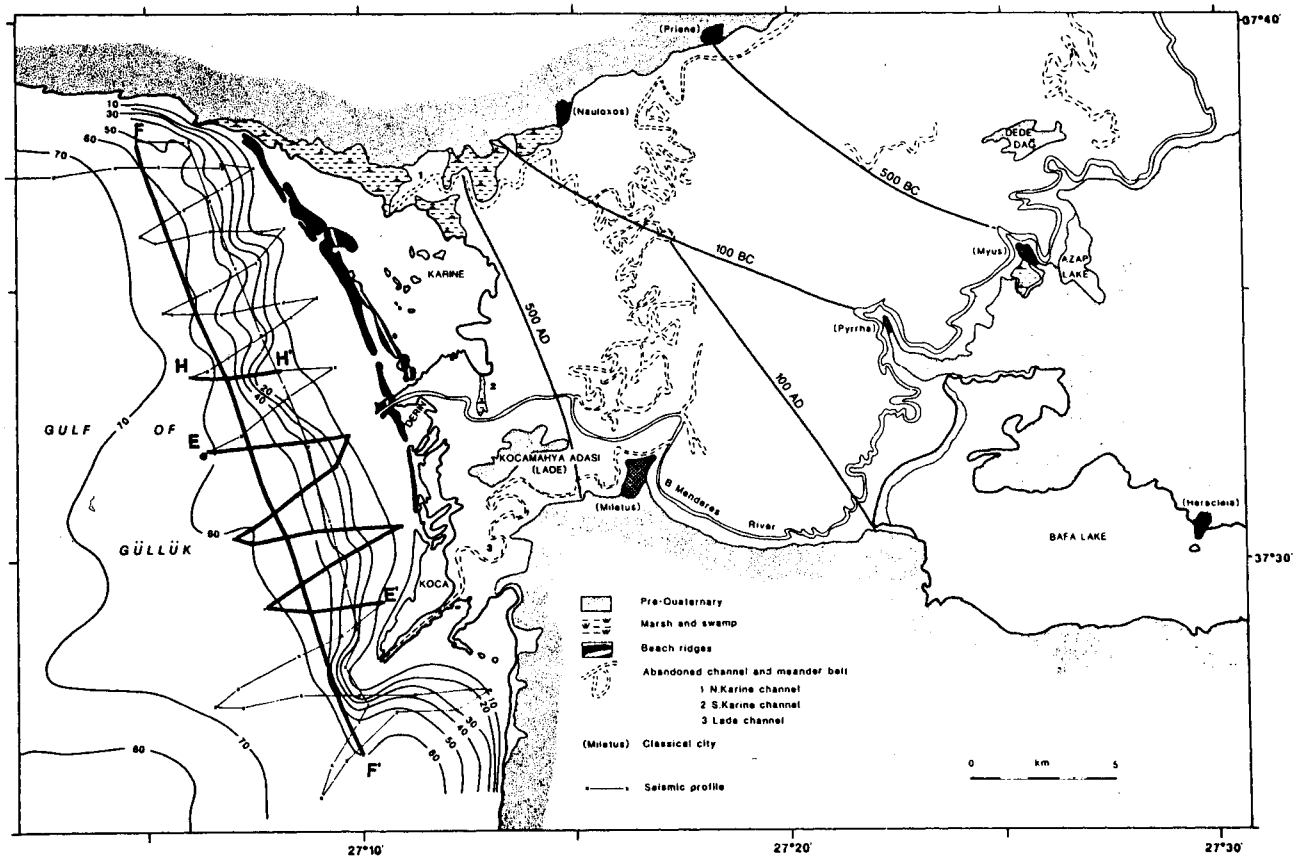

Fig. 3. Bathymetric map of the Gulf of Güllük, showing seismic profiles, core location (solid circle), present-day Büyük Menderes river, the position of former shorelines and classical Greek and Roman cities (in parantheses). Isobaths are in metres; E-E', F-F' and H-H' are seismic profiles illustrated in Figs. 10, 11 and 21, respectively.

Şekil 3. Sismik profilleri, karot alım yerlerini (içi dolu daireler), güncel Büyük Menderes Nehri, eski kıyı çizgileri ve Eski Latin şehirlerini (parantezler içerisinde) gösteren, Güllük Körfezi Batimetri Haritası. Derinlikler metre olup, E-E', F-F' ve H-H' Şekil 10, 11 ve 21'de verilen sismik profillerin yerlerini göstermektedir.

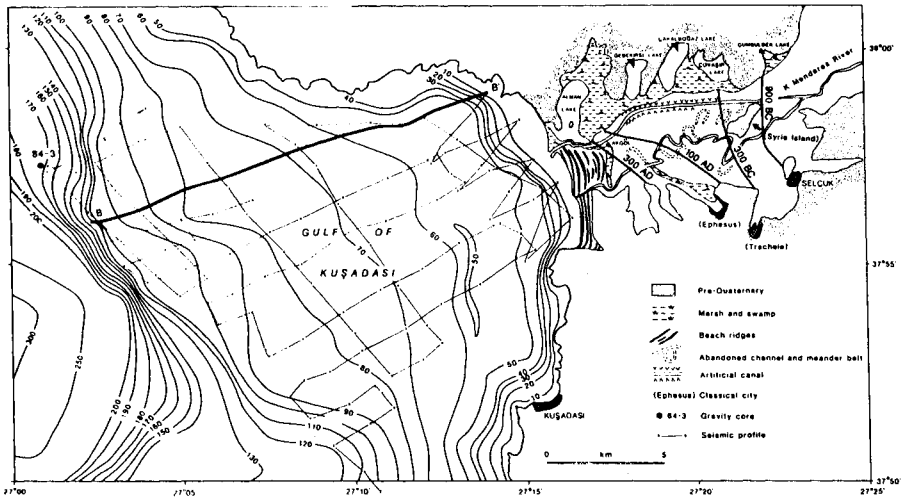

Fig. 4. Bathymetric map of the Gulf of Kuşadası showing seismic profiles, core location (solid circle), present-day Küçük Menderes river, the position of former shorelines and classical Greek and Roman cities (in parantheses). Isobaths are in metres; B-B' is seismic profiles illustrated in Fig. 7.

Şekil 4. Sismik profilleri, karot alım yerlerini (içi dolu daireler), güncel Küçük Menderes Nehri, eski kıyı çizgisi ve Eski Latin şehirlerini (parantezler içinde) gösteren Kuşadası Körfezi Batimetri Haritası. Derinlikler metre olup, B-B' Şekil 7' de gösterilen sismik profilin konumunu belirtmektedir.

sent Gediz delta has a subaqueous pro-delta platform, 1-5 km wide and less than 10 m deep which is bounded by steep slopes leading to the floor of the bay. The inner part of Izmir Bay is less than 20 m deep, and the seabed slopes gently to the northwest to about the 110 m isobath, where there is an abrupt break in slope marking the limit of late Pleistocene delta progradation. The Bakırçay river drains into the head of Çandarlı Bay and in the late Pleistocene its delta prograded westward into the fault-bounded Çandarlı Basin. The latter is an isolated bathymetric depression, located in Çandarlı Bay (Fig. 2). In the central portion the water depth exceeds 140 m and a narrow northeast-southwest trending platform, less than 95 m deep, connects Çandarlı Basin to the outer Izmir Bay. The Madra river flows into the northern Dikili Bay and during the late Pleistocene its delta prograded southward into the northern portion of the Çandarlı Basin.

The Büyük Menderes river flows into the northern part of Gulf of Güllük (Fig. 3). The continental shelf off the Büyük Menderes river is over 60 km wide and includes several smaller islands between the islands of Ikaria and Kos. The delta has a subaqueous prodelta platform 1-2.5 km wide <10 m deep with steep prodelta slopes. The shelf gradient off the Büyük Menderes is much gentler than off the Küçük Menderes and the shelf break occurs in water depths between 100 and 120 m. The Küçük Menderes river flows into the Gulf of Kuşadası (Fig. 4) where the continental shelf is generally only 4 km wide, but widens to over 15 km off the Küçük Menderes delta. The present delta has a subaqueous prodelta platform 0.5-1.5 km wide and less than 10 m deep. Steep slopes lead from the prodelta platform to about 50 m water depth, below which there is a much gentler shelf gradient. The shelf break occurs at about 110 m, with steep slopes down to the basin floor at around 400 m north of the island of Samos.

DATA COLLECTION AND METHODS

The seismic and core data that constitute the basis of this paper were collected from the research vessel Koca Piri Reis of the Institute of Marine Sciences and Technology in 1979, 1984 and 1985. In 1979, approximately 300 line-km of 3.5-kHz profile data and 5 gravity cores were collected from the outer Izmir Bay and Çandarlı Bay (Fig. 2; Table 1) and interpreted by Aksu and Piper (1983). During the 1984 survey, about 800 line-km of single-channel seismic reflection and 3.5-kHz profiles and 3 gravity cores were collected from the study area (Figs. 2,3,4; Table 1) and interpreted by Aksu *et al.* (1987a,b). The seismic data were obtained using a 40-inch^3 air-gun source and a 21-elements, 9-m-long hydrophone streamer. The signal was bandpass filtered to the 60-800 Hz range. During the 1985 survey, about 400 line-km of 3.5-kHz and 200 line-km of side-scan sonar profiles and 7 gravity cores were collected from the Çandarlı and Dikili Bays (Fig. 2; Table 1).

Cores were obtained using a benthos gravity corer with 8.9 cm internal diametre. Cores collected in 1979 and 1984 were air freighted to Canada, where they were split, X-rayed and centimetre by centimetre visual descriptions were made to determine stratification, primary and secondary sedimentary structures and coring disturbances. Colours of the wet sediment surface were determined using Geological Society of America Rock Colour Chart. Cores collected in 1985 were immediately split and described on board the research vessel Koca Piri Reis and continuous, 1 cm thick, sediment slabs were taken from the cores. These slabs were air freighted to Canada where they were X-rayed and further described. Selected cores were sampled for sedimentological, geochemical and micropaleontological studies. Quaternary to Recent foraminifera were separated, identified and counted following the methods described by Aksu (1981). Stable isotopic determinations in foraminifera were carried out following the technique described in Aksu (1985). Grain size analyses were carried out using standard sieving and pipetting the >63μm and <63μm fractions, respectively. Heavy minerals were identified under polarizing microscope in 2.5-3.0 Φ fractions and clay minerals were identified based on their basal diffraction peaks in <2μm fractions.

Table 1. Location, water depth and length of cores used in this study

Çizelge 1. Bu çalışmada kullanılan karotların alındıkları koordinatlar, su derinlikleri ve uzunlukları

CORE	LATITUDE (N)	LONGITUDE (E)	DEPTH (m)	LENGTH (cm)
79-1	38°43'23"	26°33'24"	88	30
79-2	38°44'06"	26°33'00"	95	125
79-3	38°44'12"	26°33'00"	103	75
79-4	38°45'01"	26°32'48"	112	92
79-5	38°46"36"	26°32'45"	140	130
84-1	38°51'00"	26°46'20"	141	206
84-2	37°32'00"	27°06'25"	172	193
84-3	37°57'18"	27°01'06"	63	130
85-1	38°43'30"	26°28'57"	129	144
85-2	38°54'58"	26°59'01"	15	50
85-3	38°54'57"	26°59'00"	15	157
85-4	38°53'17"	26°50'10"	100	159
85-5	38°52'58"	26°58'00"	53	192
85-6	38°50'30"	26°46'30"	140	201
85-7	38°51'03"	26°43'00"	112	59

OCEANOGRAPHY

The mean tidal range along the eastern Aegean Sea is only 20 cm, with a spring tide of up to 70 cm. During storm conditions the range between highest high water and lowest low water at Kuşadası may be as much as 100 cm. At Kuşadası the average wave height and length are 0.6 and 150 m respectively with storm waves reaching about 3 m in height and 50-70 m in length. Field observation in 1983 suggested that below 20 m water depth the winnowing effect of waves is negligible. Little data exist on the water circulation patterns in the Gulfs of Kuşadası and Güllük.

The surface water circulation in Izmir Bay is variable as the result of the prevailing winds in the area. In the summer and autumn the surface water is driven by NW and WNW winds toward the southeast paralleling the coastline with speeds of about 40 cm s^{-1}. In the winter, the winds are from the N and NE and the currents are toward the south with speeds of 30 cm s^{-1}. There is no predominant surface current direction in the spring and measurements show consierable reduction in current speeds (6-20 cm s^{-1}). Sparce available data suggest that the bottom currents in Izmir Bay move reciprocally to the surface water.

RIVERS

(1) Gediz river

The Gediz river drains a basin of 15616 km^2 with an annual discharge ranging from 40 to 70 m^3 s^{-1} (Fig. 5). In its

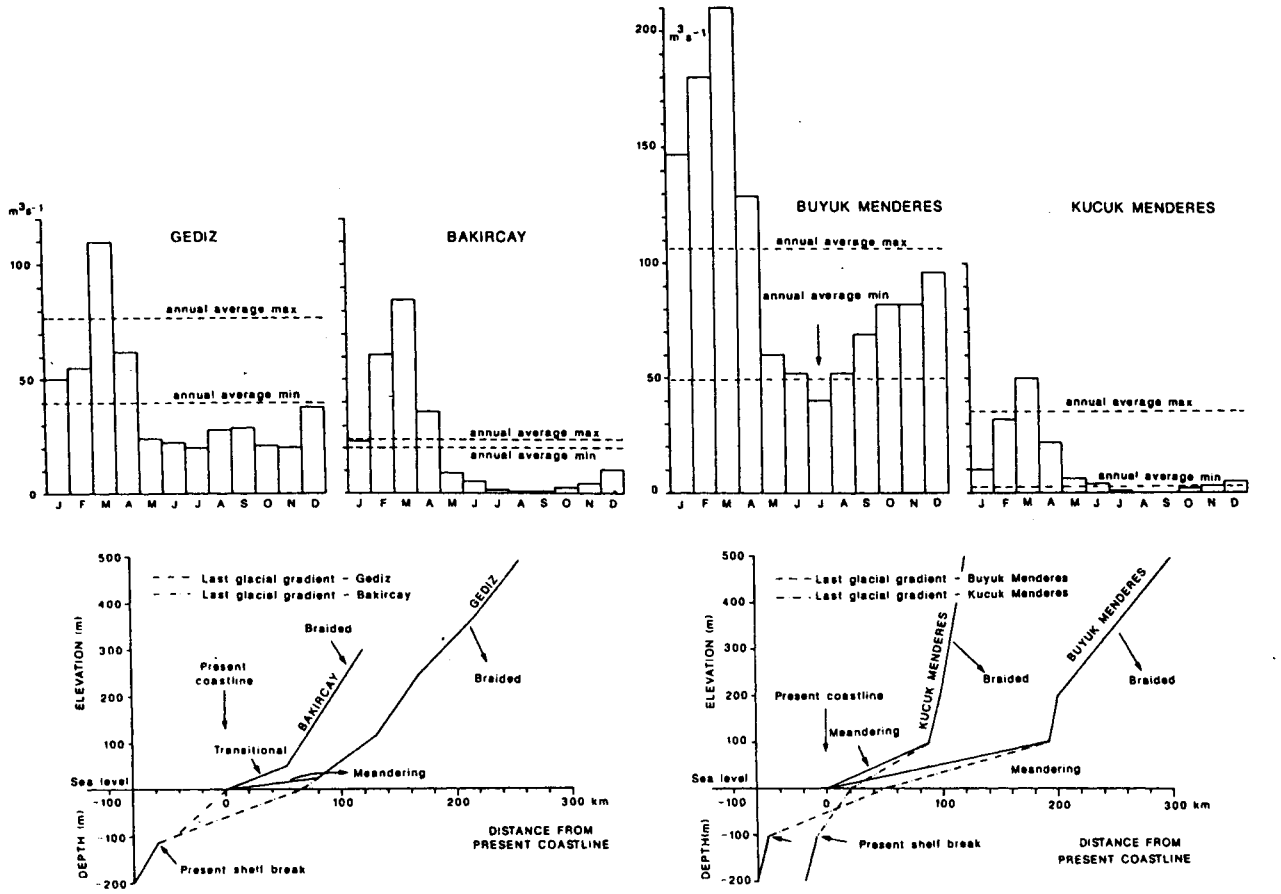

Fig. 5. Monthly average discharge rates ($m^3 s^{-1}$) for Gediz, Bakırçay, Büyük Menderes and Küçük Menderes rivers; data from Unesco (1969) and Topraksu (1980). Also shown are present and inferred Pleistocene gradients for the rivers.

Şekil 5. Unesco (1969) ve Topraksu (1980) den alınmış Gediz, Bakırçay, Büyük Menderes ve Küçük Menderes Nehirlerinin aylık ortalama debileri (m^3/sn) ile güncel ve Pleyistosen (teorik) nehir grafikleri.

middle reaches, the channel gradient is about 1:400 and the river is braided. The lower 80 km of the river is meandering, with a channel gradient of 1:3200. The construction of the Demirköprü dam in 1960 and the subsequent irrigation network have significantly altered the hydraulic regime of the Gediz river. The suspended sediment discharge of the Gediz river between November and March is about 2.5 kg m^{-3}. (Saatçi and Taysun 1979). This figure suggests an average sediment discharge varying between 100 and 190 kg s^{-1}, and an annual sediment yield of between 3.2 and 6.1 million tonnes.

(2) Bakırçay river

The Bakırçay is a considerably smaller river, draining a basin of 2888 km^2. At about 20 km landward of its present mouth, the annual average discharge of the river varies between 19 and 23 $m^3 s^{-1}$, but for the four summer months it is almost dry (Fig. 5). The channel gradient in the middle reaches is about 1:260 and the river is braided. In its lower reaches the gradient decreases to 1:1000 and the channel has a transitional braided to meandering pattern, reverting to meadering on the last few kilometres of its course. The Bakırçay river is not dammed and little data exist on the suspended sediment discharge.

(3) Madra river

Madra is a very small river, draining a basin of about 1590 km^2. At its present mouth, the annual average discharge of the river ranges from 5 to 12 $m^3 s^{-1}$, and the river is completely dry during the summer months. In its upper and middle reaches the river is braided, but meanders only on the last 1-3 km of its course. Little data exist on the suspended sediment discharge rates of the Madra river.

(4) Büyük Menderes river

The Büyük Menderes river drains a basin of 23889 km^2 with an average annual discharge of 90 $m^3 s^{-1}$ (Fig. 5; Unesco 1969). About 70% of this discharge occurs between November and March, correlating closely with the precipitation patterns of the region. The suspended sediment discharge of the Büyük Menderes river is about 3 kg m^{-3} (EIEI 1981), which suggests an average annual sediment discharge of 270 kg s^{-1}, and an annual sediment yield of 8.5 million tonnes.

(5) Küçük Menderes river

The Küçük Menderes river drains a small basin (about 3255 km^2) with an annual discharge of 17 $m^3 s^{-1}$ (Fig. 5). The suspended sediment discharge of the river below the confluence of all major tributaries is about 0.6 kg m^{-3}, suggesting an annual sediment discharge of 10 kg s^{-1}, and an average sediment yield of about 0.5 million tonnes per year. The construction of a canal in 1934 (Fig. 4) and the subsequent irrigation network have significantly altered the hydraulic regime of the Küçük Menderes river. Both Büyük and Küçük Menderes riv-

ers are braided in their upper reaches, becoming meandering on their flat delta plains.

DELTAS

The subaerial morphologies of these deltas are similar to that of other eastern Mediterranean deltas (Russell 1954, Piper and Panagos 1979) and show alluvial drowning along their lower courses.

(1) Gediz delta

The areal extent of the Gediz delta is about 500 km^2 and shows phases of lobate and elongate delta progradation. Deposits in the lower parts of the river are meander-belt sands and flood basin muds, and the present delta is made up of one lobe, fed by two distributaries. The southern shore of the delta consists of abandoned channels, extensive marshes and swamps, and small islands and inlets. The northern shore of the delta includes barrier islands and bars formed by reworking and redistribution of progradational channel mouth deposits are extensive lagoons, lakes, small islands and salt marshes. On the delta plain there are six major abandoned channels that suggest the development of several sub-deltas during the Holocene (Erinç 1955). These channels are: Mirmekes, Değirmentepe, Maltepe, Kokala, Karşıyaka and Pelikan. The submarine morphology of the Holocene Gediz delta is discussed in detail by Aksu and Piper (1983).

The tentative successive positions of the shoreline resulting from the late Holocene delta progradation are illustrated in Figure 2. At about 1000 BC the coastline lay immediately west of Larissa. By 500 BC it prograded westward to a line from Leucea to Menemen. At about 100 AD the coastline lay south of Leucea and at around 1000 AD the entire ancestral bay was filled by the progradational deltaic sediments, except for a narrow strip east of the Pelikan Bank.

(2) Bakırçay delta

The areal extent of the Bakırçay delta is about 100 km^2. Deposits in the lower course of the river are channel sands and flood basin muds. The present delta is made up of one lobe fed by two distributaries (Fig. 2). The shore of the delta includes a few abandoned channels, extensive marshes and swamps and small islands and lakes. The subaqueous delta platform is about 750 m wide and less than 10 m deep and it is bounded by steep prodelta slopes.

Little data exist on the progradational history of the Holocene Bakırçay delta. The classical Aeolian city of Elaea was built on the promontory of the coast by the sea. By 100 AD the coastline was located about 2.6 km southwest of the river mouth. Today Elaea is situated approximately 5 km inland from the present shoreline.

(3) Madra delta

The areal extent of the Madra delta is about 25 km^2 and the present delta is fed by a single distributary. The shore of the delta consists of extensive beach ridges, probably formed by the reworking of the channel mouth coarse clastics by waves and currents. The subaqueous prodelta platform is approximately 500 m wide and less than 10 m deep with relatively gentle slopes leading to northern Dikili Bay. No data is available on the subareal progradational history of the Holocene Madra delta.

(4) Büyük Menderes delta

Büyük Menderes delta is about 600 km^2. The lower reaches of the river are characterized by an elaborate network of abandoned meandering channels and extensive flood basins (Fig. 3). The construction of irrigation canals and a dam (between 1960-1980) helped regulate the flow regime of the river, largely eliminating severe winter flooding. A coastal barrier island system extends for the entire width of the Büyük Menderes delta, developed by reworking of coarse channel mouth clastics by waves and longshore currents. Landward of the barrier islands and bars are extensive lagoons, lakes, swamps and marshes. The present delta is made up of one lobe, fed by a single channel. On the delta plain, there are several abandoned channels that suggest the development of several subdeltas.

Holocene delta progradation can be inferred from archaeological and historical data (Erinç 1978, Aksu *et al.* 1987b). The tentative successive positions of the shoreline are shown in Figure 3. At 500 BC it lay 20 km inland, between Priene and Myus. By 100 BC it had prograded 5-8 km, particularly in the north, to a line from Nauloxos to Pyrrha. About 200 years later (100 AD) progradation in the south had closed the entrance of the Latmian Gulf. By 500 AD the coastline was seaward of Miletus, some 5 km from the present costline.

(5) Küçük Menderes delta

The areal extent of the Küçük Menderes delta is about 50 km^2, and it is connected to the inner Küçük Menderes flood plain by a relatively narrow valley, NE of Selçuk (Fig. 4). Lakes, swamps and marshes cover nearly the entire delta plain north of the 1934 canal. South of the canal, the delta plain includes meander belt sands, flood basin muds and abandoned channels. Two semi-permanent lakes are conspicuous in the delta plain; the Akgöl is about 40 cm below the present sea-level and represents an older distributary of Küçük Menderes (Erinç 1955). The other swamp lies NW of the classical town of Ephesus and represents the ancient harbour which was dredged numerous times in desperate efforts to save the town (Bean 1966, Erinç 1978). The shore of the delta consists of extensive beach ridges and coastal dunes, formed by reworking and redistribution of progradational channel mouth deposits. These beach ridges were formed between approximately AD 100 and 1934, and after the construction of the canal in 1934 a new beach-ridge was formed north of the canal mouth (Eisma 1978).

The late Holocene delta progradation can also be inferred from historical and archaeological data. This progradation sequence is illustrated in Figure 4. There appears to have been a rapid delta progradation from a shoreline near Syrie Island about 900 BC to close to its position by 300 AD. Since that time successive beach ridges have accreted at the delta shoreline.

SEISMIC STRATIGRAPHY

Both air-gun and 3.5 kHz seismic profiles show prograding sigmoidal wedges of sediment immediately seaward of all five deltas studied (Figs. 6, 7), and are referred to as Holocene deltas, without implying precise chronostratigraphic connotation. Around the shelf break area seaward of the Gediz, Bakırçay, Madra and Küçük Menderes deltas, seismic profiles also show a number of superimposed prograding oblique sediment wedges (Figs. 6, 7, 8, 9). These can be traced landward to beneath the modern delta where they are largely obscured by the bottom multiple. Underlying the modern Büyük Menderes delta, a similer sequence of stacked deltas can be recognised (Figs. 10, 11). These deltaic sequences are referred to as Pleistocene deltas.

The air-gun seismic profiles are divided into depositional sequences on the basis of widespread correlatable reflections, reflection groups and unconformities. This technique is fully discussed in Mitchum *et al.* (1977), and briefly described here. A depositional sequence is defined as a seismic strati-

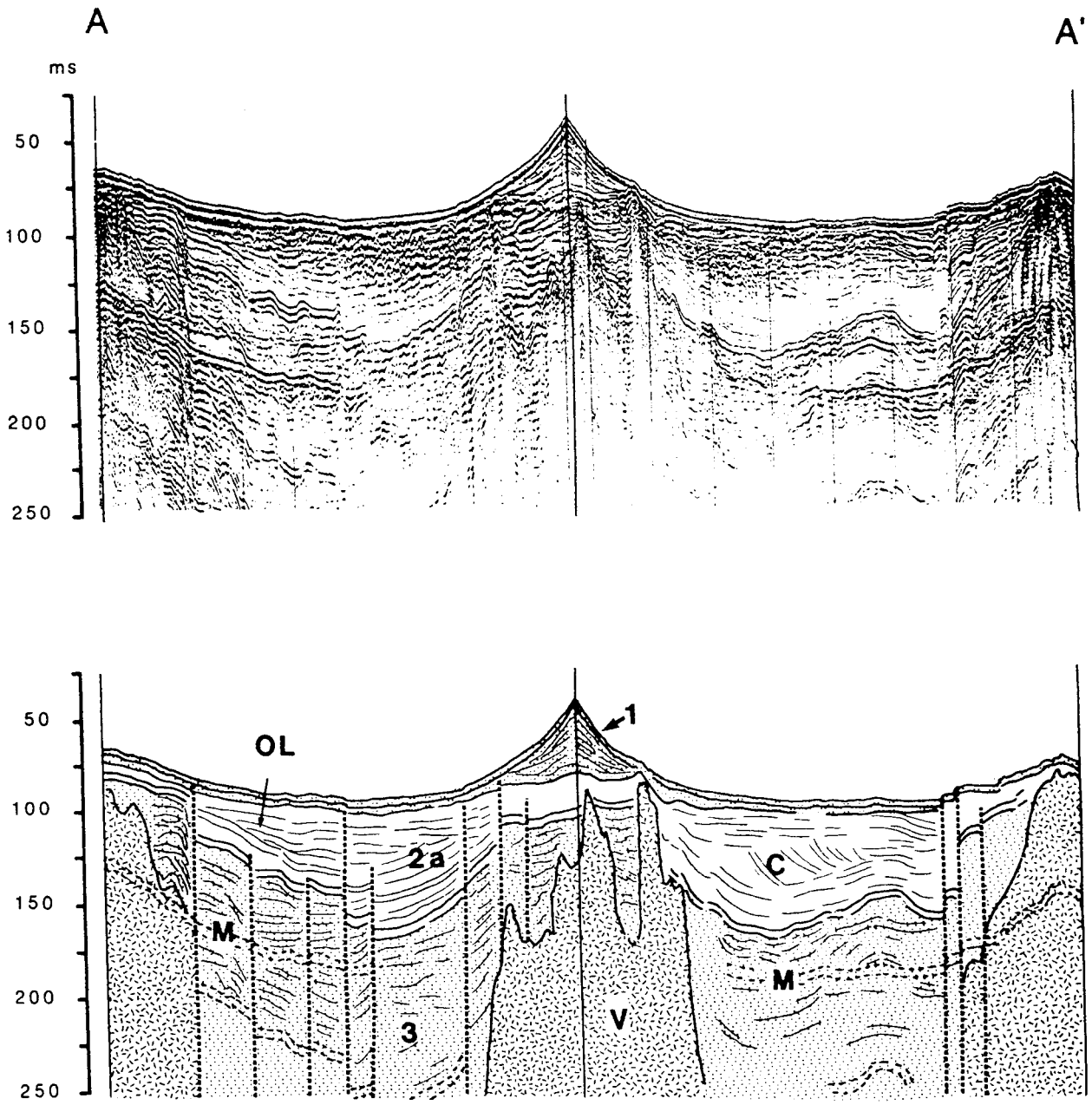

Fig. 6. Air-gun seismic profile (A-A') across Izmir Bay. Location is shown in Figure 2. 1 to 3 are depositional sequences; 2A is the depositional sequence related to the progradation of Gediz delta. OL= onlap, C= clinoforms, V= volcanics, M= multiple, dashed lines = faults. Profile is about 32 km long, vertical exaggeration= 64.

Şekil 6. Konumu Şekil 2'de gösterilen İzmir Körfezi'ne ait hava tabancası sismik profili (A-A'). 1-3 depolanma istifleri olup, 2A Gediz Deltasının ilerleyişi ile ilişkili olan depolanma istifidir. OL= onlap, C= klinoform, V= volkanikler, M= tekrarlı yansımalar, kesikli çizgiler= faylardır. Profil uzunluğu 27 km ve düşey abartma 64'tür.

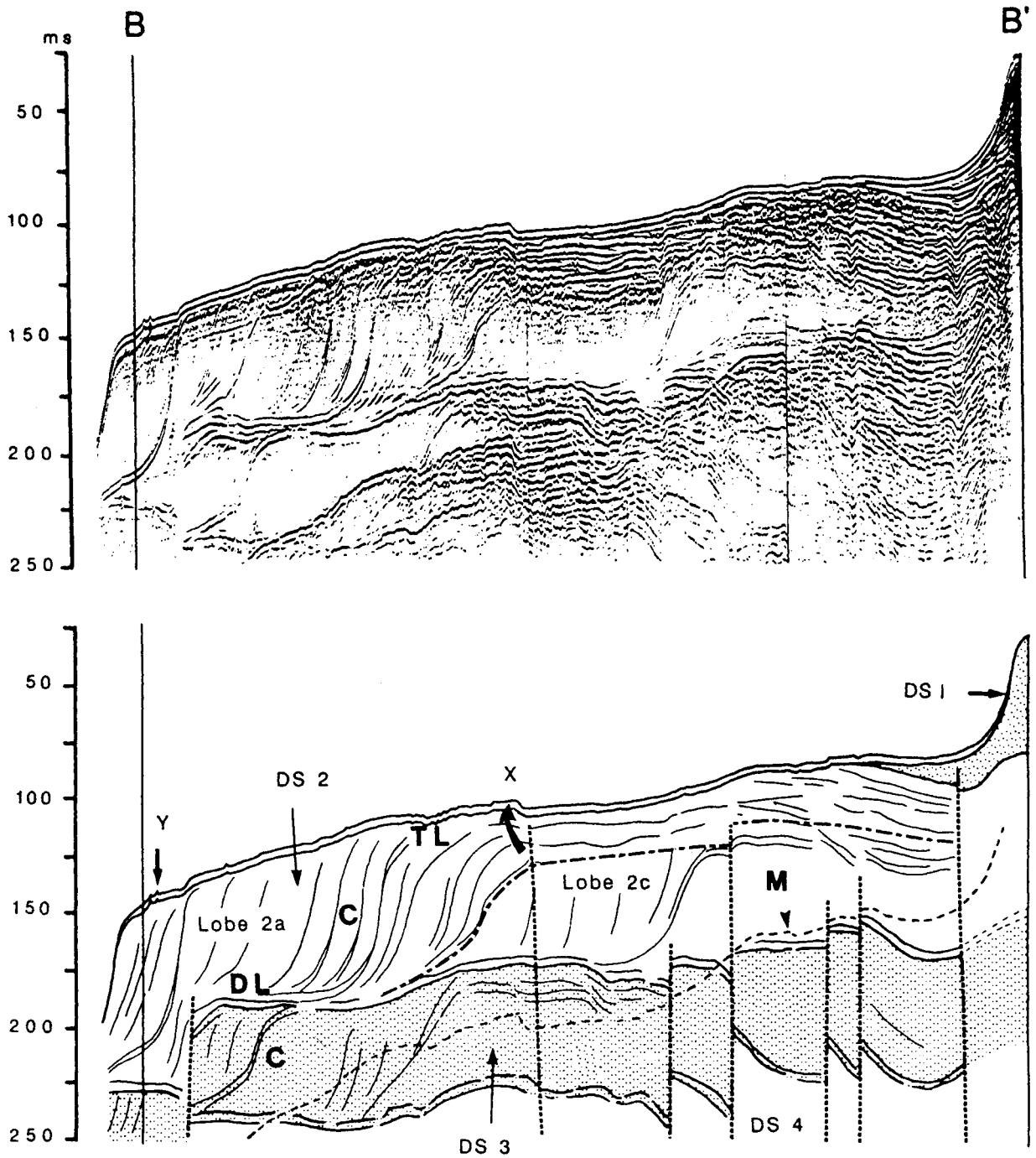

Fig. 7. Air-gun seismic profile (B-B') across the Gulf of Kuşadası. Location is shown in Figure 4. 1 to 4 are depositional sequences. C=prograding clinoforms, TL= toplap, DL=downlap, M= Multiple, dashed lines= faults. Lobes 2A and 2C, X and Y explained in text. Profile is about 27 km long, vertical exaggretaion= 66.

Şekil 7. Konumu Şekil 4'de gösterilen Kuşadası Körfezine ait hava tabancası sismik profili (B-B'). 1-4 depolanma istifleridir. C= ilerleme klinoformları, TL= toplap, DL= downlap, M= tekrarlı yansımalar, kesikli çizgiler= faylardır. 2A ve 2C lobları ile X ve Y metin içerisinde açıklanmıştır. Profil uzunluğu 27 km olup, düşey abartma 66'dır.

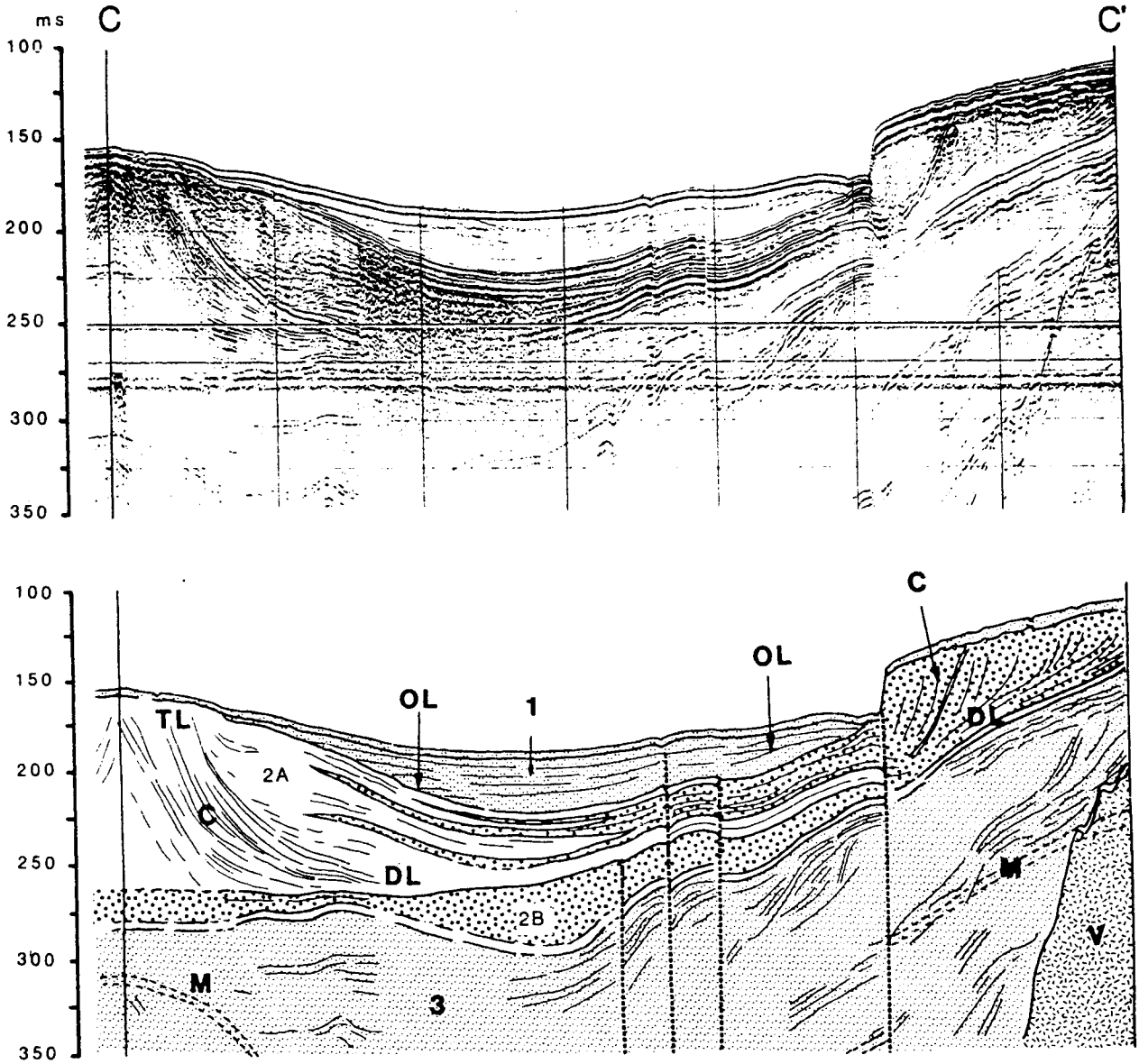

Fig. 8. Air-gun seismic profile (C-C') across the Çandarlı Basin. Location is shown in Figure 2. 1 to 3 are depositional sequences; 2A and 3B are depositional sequences related to the progradations of Gediz and Bakırçay deltas, respectively. OL= onlap, TL= toplap, DL= downlap, C= clinoforms, M= multiple, V= volcanics, dashed lines= faults. Profile is about 15 km long, vertical exaggeration= 34.

Şekil 8. KonumuŞekil 2'de gösterilen Çandarlı Havzasına ait hava tabancası sismik profili (C-C'). 1-3 depolanma istifleri olup, 2A ve 2B Gediz ve Bakırçay deltalarının ilerlemesiyle ilişkili depolanma istifleridir. OL= onlap, TL= toplap, DL= downlap, C= klinoformlar, M= tekrarlı yansımalar, V= volkanikler, kesikli çizgiler= faylardır. Profil yaklaşık 15 km uzunluğunda olup, düşey abartma 34'tür.

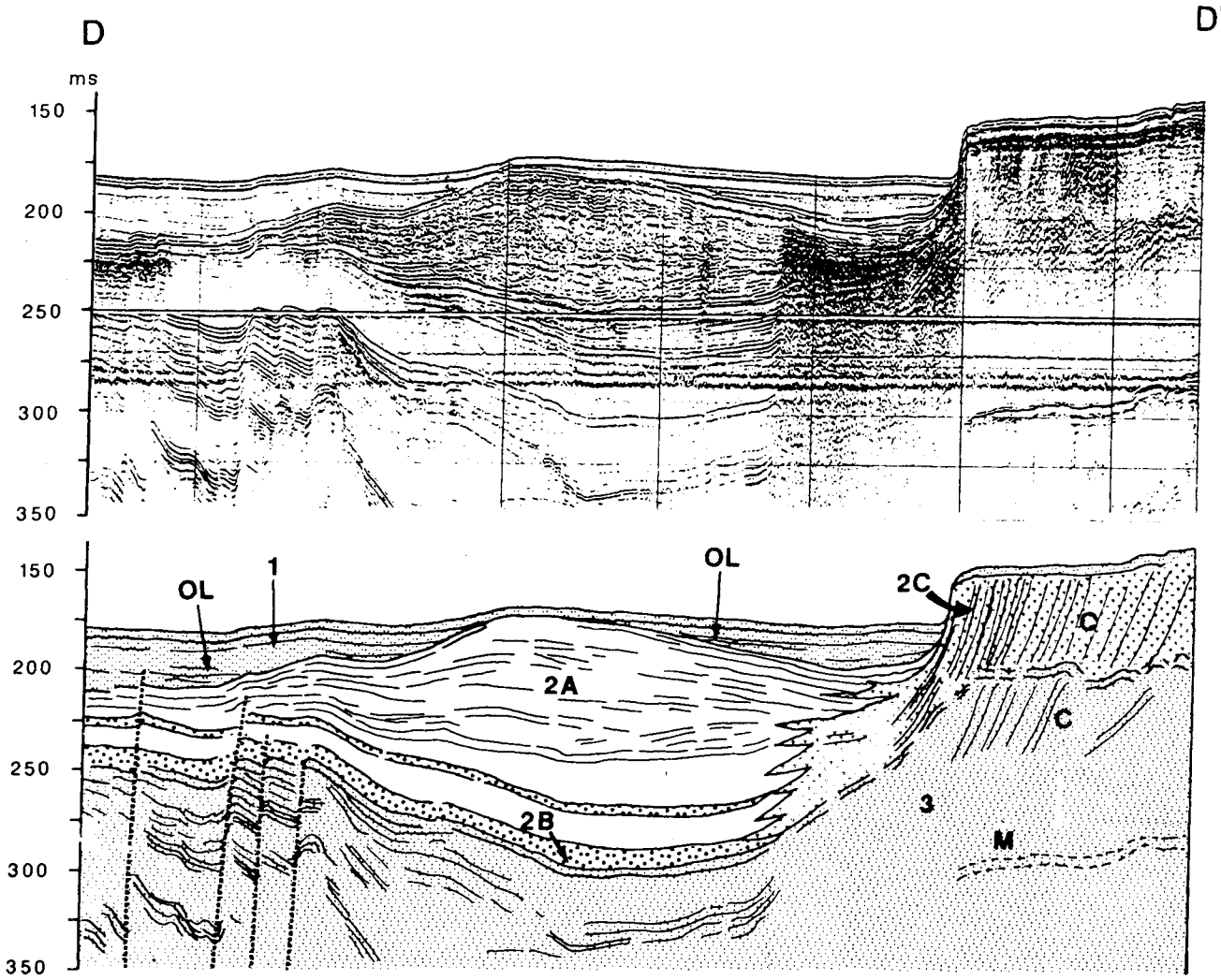

Fig. 9. Air-gun seismic profile (D-D') across the Çandarlı Basin. Location is shown in Figure 2. 1 to 3 are depositional sequences; 2A, 2B and 2C are depositional sequences related to the progradations of Gediz, Bakırçay and Madra deltas, respectively. OL= onlap, C= clinoforms, M= multiple, dashed lines= faults. Profile is about 12 km long, vertical exaggeration= 35.

Şekil 9. Konumu Şekil 2'de gösterilen Çandarlı Havzasına ait hava tabancası sismik profili (D-D'). 1-3 depolanma istifleri olup, 2A, 2B, ve 2C sırasıyla Gediz, Bakırçay ve Madra Deltalarının ilerlemesiyle ilişkili depolanma istifleridir. OL= onlap, C= klinoformlar, M= tekrarlı yansımalar, kesikli çizgiler= faylardır. Profil uzunluğu 12 km ve düşey abartma 35'dir.

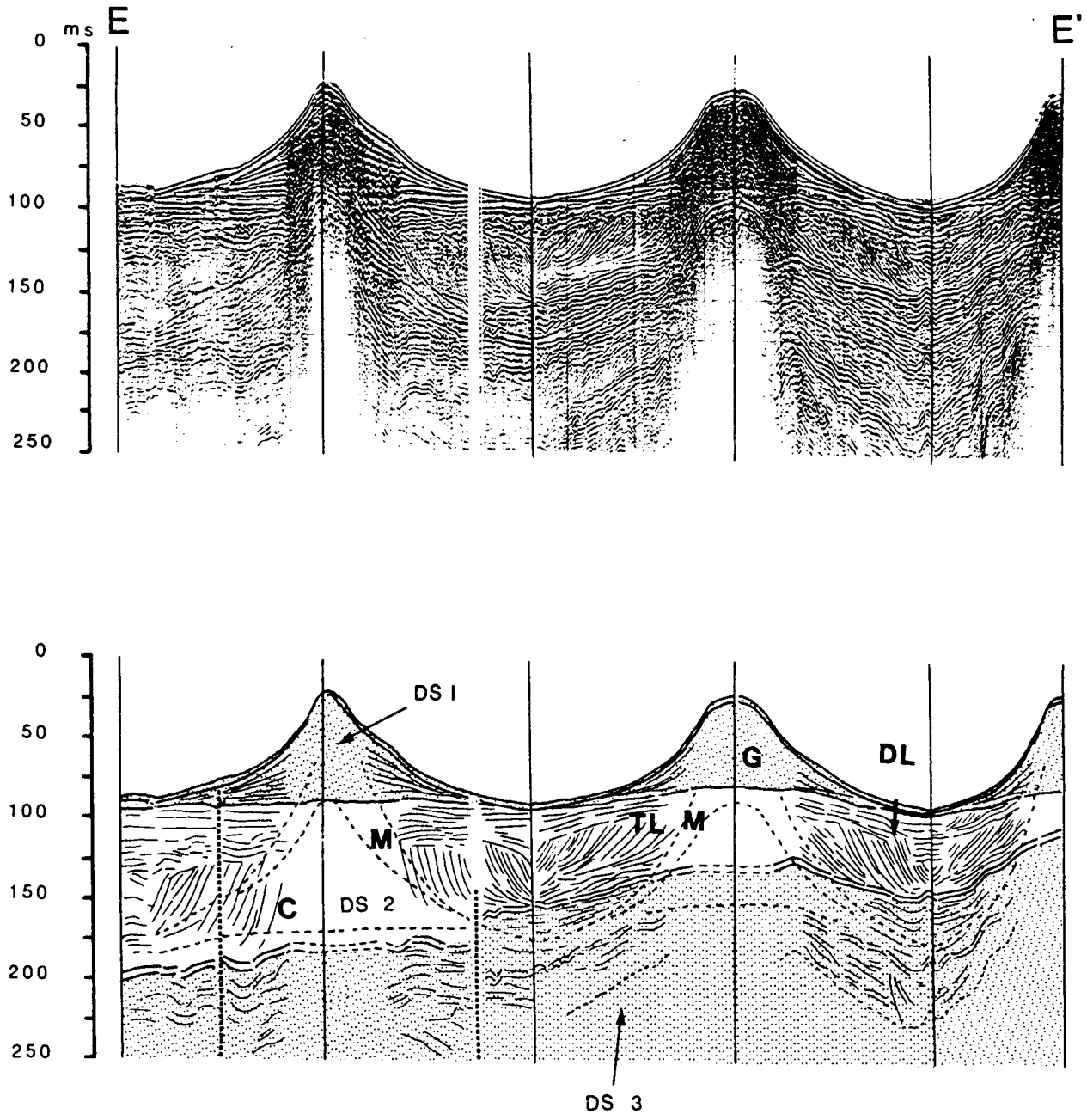

Fig. 10. Air- gun seismic profile (E-E') off the Büyük Menderes delta. Location is shown in Figure 3. 1 to 3 are depositional sequences. C= prograding clinoforms, TL= toplap, DL= downlap, G= gas charged sediments, M= multiple; dashed lines= faults. Profile is about 32 km long, vertical exaggeration= 80.

Şekil 10. Konumu Şekil 3'de gösterilen Büyük Menderes Deltasına ait hava tabancası sismik profili (E-E'). 1-3 depolanma istifleridir. C= İlerleyen klinoformlar, TL= toplap, DL= downlap, G= gaz yüklü sedimentler, M= tekrarlı yansımalar, kesikli çizgiler= faylardır. Profil uzunluğu 32 km ve düşey abartma 80'dir.

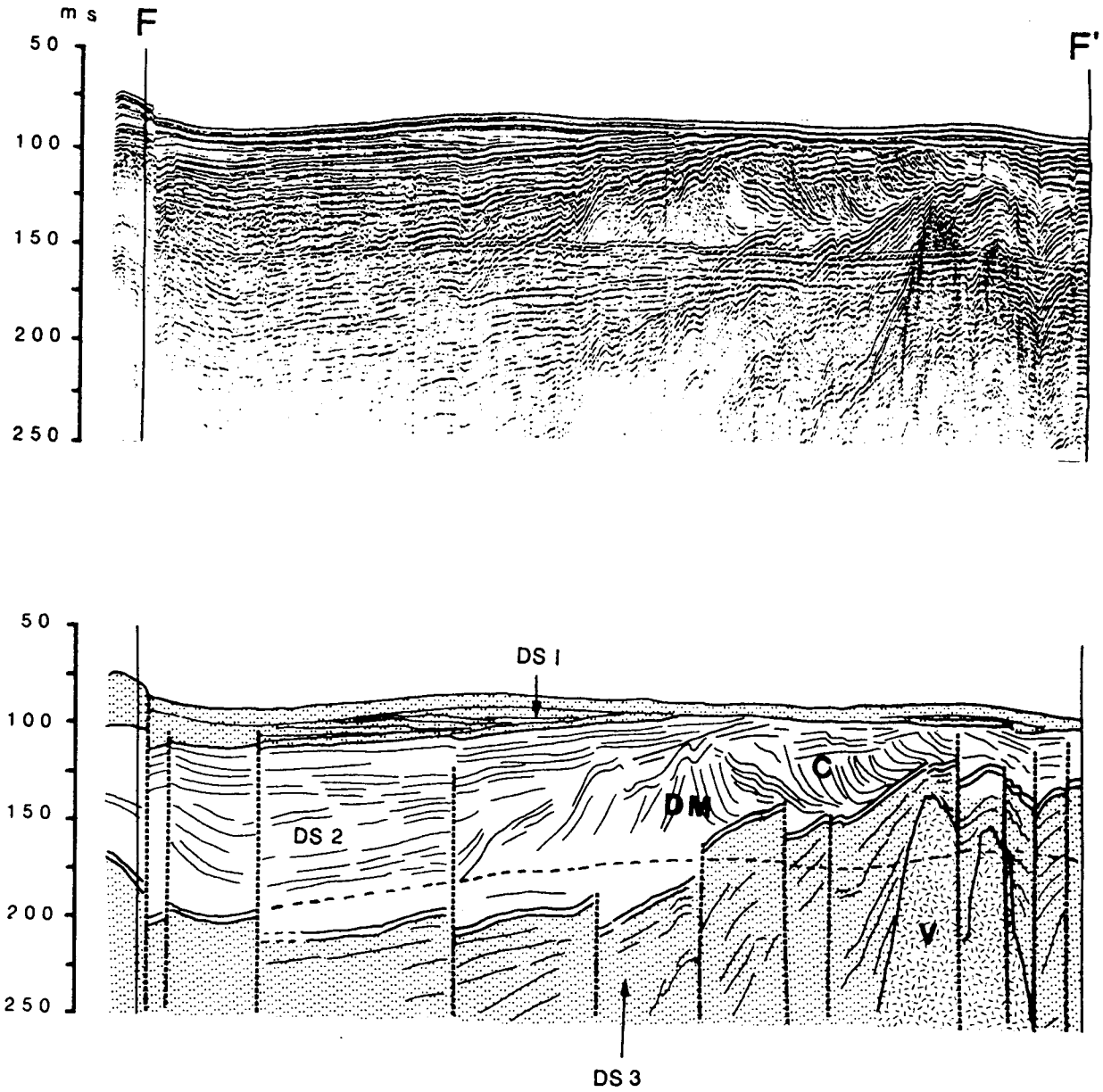

Fig. 11. Air-gun seismic profile (F-F') across the Büyük Menderes delta. Location is shown in Figure 3. 1 to 3 are depositional sequences. V= intrusive rock, C= prograding clinoforms, DM= depositional mouth; dashed lines= faults. Profile is about 22 km, vertical exaggeration= 78.

Şekil 11. Konumu Şekil 3'de gösterilen Büyük Menderes Deltasına ait hava tabancası sismik profili (F-F'). 1-3 depolanma istifleri olup, V= volkanikleri, C= ilerleme klinoformlarını, DM= depolanma ağzını, kesikli çizgiler= fayları göstermektedir. Profil uzunluğu 22 km, düşey abartma ise 78'dir.

graphic unit consisting of genetically related, conformable reflectors that are bounded at its top and/or base by unconformities. In most seismic profiles the determination of unconformities is based upon toplap and downlap reflection terminations on the upper or lower boundary. However, in basinal sediments, such as Çandarlı Basin and outer Izmir Bay, reflectors extended over long distances without apparent terminations. In these areas where toplap and downlap are not readily identified, the nearest widespread correlatable reflector is taken as the depositional sequence boundary.

(1) Gediz, Bakırçay and Madra seismic sequences

Four depositional sequences are identified in the outer Izmir Bay and Çandarlı Bay:

Depositional sequence 1

Except in the Çandarlı Basin, depositional sequence 1 is a sigmoidal seismic unit consisting of seaward prograding clinoforms (Fig. 6). Depositional sequence 1 occurs immediately seaward of the modern Gediz, Bakırçay and Madra deltas (Fig. 12). In seismic profiles proximal to inferred river mouths, reflectors commonly exhibit downlap and offlap terminations. The latter is probably formed by seaward thinning of strata to less than the resolution of the acoustic system.

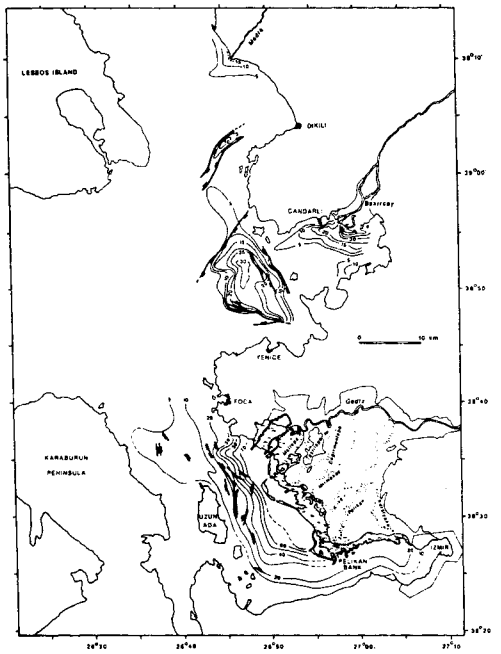

Fig. 12. Isopach map of Depositional Sequence 1 in the Gediz, Bakırçay and Madra deltas, showing sediment thickness in milliseconds two-way travel time. Heavy lines are faults with ticks on downthrown side. Acoustic source: air-gun, except 3.5 kHz in the Dikili Bay. Depositional Sequence 1 correlates with the seismic units I to IV of Aksu and Piper (1983).

Şekil 12. Gediz, Bakırçay ve Madra Deltalarına ait 1 nolu depolanma istifi Eşkalınlık Haritası. Sediment kalınlığı milisaniye olarak gidiş-geliş zamanı olup, kalın çizgiler fayları göstermektedir. Akustik kaynak, Dikili körfezinde çalışılan 3.5 kHz'in dışında hava tabancasıdır. 1 nolu depolanma istifi Aksu ve Piper (1983)'ün 1 ve IV no'lu sismik birimleriyle ilişkilidir.

Seismic correlation shows that a thick accumulation in the Çandarlı Basin is the distal equivalent of depositional sequence 1. Here, the sequence exhibits weak, internally parallel reflectors that gently onlap the underlying reflectors (Fig. 8). The onlapping character of this sequence, that fills negative relief areas, indicates deposition from low velocity, gravity driven density flows (Aksu and Piper 1983). The distributional pattern of the depositional sequence 1 off the Madra river show the presence of a small and broad delta lobe, confined mostly to the present day river mouth, rapidly thinning westward and southward (Fig. 12). This pattern suggests that little or no sediment by-passed the shelf break at the northern periphery of the Çandarlı Basin. The distribution pattern of depositional sequence 1 off the Bakırçay river shows a broad wedge of sediment that rapidly thins towards the west, forming an elongate lobe immediately east of Çandarlı Basin (Fig. 12). This pattern strongly suggests that the sediments of depositional sequence 1 in Çandarlı Basin are supplied from the Bakırçay river, possibly related to episodic heavy precipitation events on land. During the associated large fluvial discharge, finer sediments may have by-passed the narrow prodelta platform and flowed into the Çandarlı Basin as density currents.

Detailed examination of the 3.5 kHz profiles shows that four depositional sub-lobes can be recognised within the depositional sequence 1 of the Gediz delta (Figs. 13, 14). All sublobes show sigmoid progradational seismic configuration. The oldest sub-lobe 1d occurs between Homa lagoon and the present Gediz mouth (Fig. 13a). It is related to the Maltepe channel and sediments within this sub-lobe probably represent proximal deltaic sedimentation and the position of the shoreline was probably comparable to that of the present day. Sublobe 1c overlies sub-lobe 1d, and occur between the Pelikan Bank and the Homa lagoon (Figs. 13b, 14). The distribution and thickness of this sub-lobe suggest that the river discharge occurred somewhere between the Kırdeniz and Kokala channels. The Mirmekes channel is the most likely channel for the observed sediment distribution. These sediments probably represent distal deltaic sedimentation and the Mirmekes mouth was probably in the northeastern part of the delta, several kilometres landward of the present shoreline. This sub-lobe may correspond to the progradation phase about 2000 yr BP that changed Leucae from an island port to an inland town (Aksu and Piper 1983).

A broad delta sub-lobe, 1b, overlies sub-lobe 1c (Figs. 13c, 14). It is thickest northwest of the Pelikan Bank (60 ms) with steep prodelta slopes down to the floor of the bay where it is only about 5 ms. Sub-lobe 1b has two major sediment accumulations (Fig. 13c 14), the oldest of which is confined to the southern part of the delta and is related to the Kokala channel. The younger accumulation is restricted to the Kokala channel. The younger accumulation is restricted to the northern part of the delta off Homa lagoon, and it is correlated with the Değirmentepe channel (Fig. 13c).

Sub-lobe 1a includes three major sediment accumulations (Figs. 13d, 14). The youngest accumulation occurs only off the present Gediz mouth and show clear progradation over the underlying older accumulation. It is therefore, correlated with deposition from the Gediz and Kırdeniz mouths since 1886 AD (Aksu and Piper 1983). An up to 20 ms thick sediment accumulation is found encircling the Pelikan Bank, with steep slopes to the south and gentler slopes to the northwest (Figs. 13d, 14). This sediment accumulation is correlated with the Pelikan channel prior to 1886 AD. A third sediment accumulation is observed in the inner Izmir Bay, and it is related to deposition from the Karşıyaka channel (Fig. 13d). Details of the Holocene delta is fully discussed by Aksu and Piper (1983).

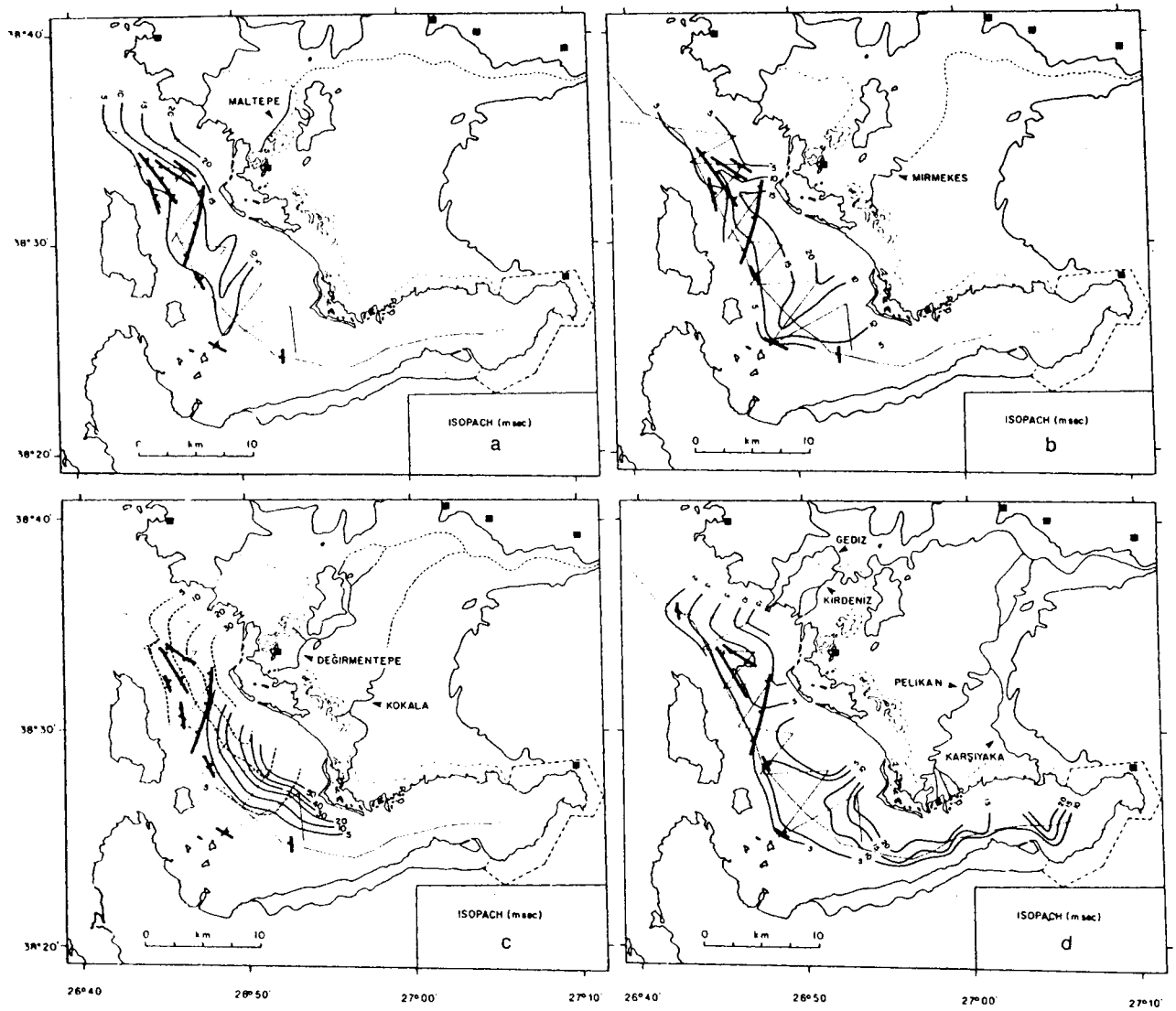

Fig. 13. Isopach maps of sub-lobes 1a to 1d in Gediz delta showing sediment thickness in milliseconds two-way travel time. Heavy lines are faults, with ticks on downthrown side. Acoustic source: 3.5 kHz.

Şekil 13. Gediz Deltasına ait 1a-1d alt-lobları Eşkalınlık Haritaları, sediment kalınlığı milisaniye olarak gidiş-geliş zamanıdır. Faylar kalın çizgilerle işaretlyenmiş olup akustik kaynak 3.5 kHz'dir.

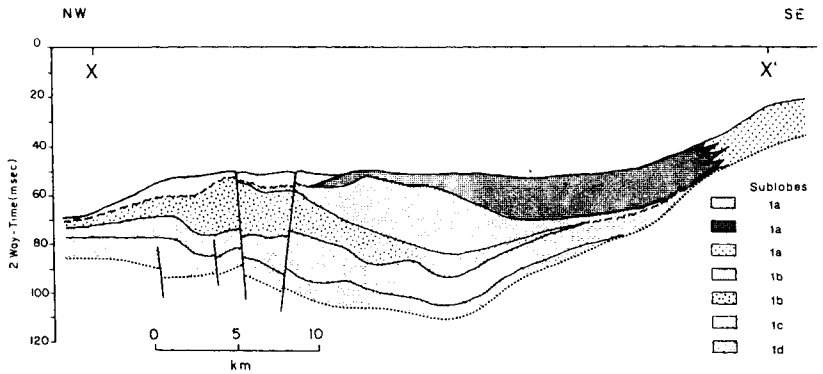

Fig. 14. Schematic NW-SE cross-section of Holocene Gediz delta showing the stratigraphic relationship of seismic sublobes. Location in Fig. 2.

Şekil 14. Sismik alt-lobların stratigrafik ilişkisini gösteren ve konumu Şekil 2'de verilen Holosen-Gediz Deltasının NW-SE yönlü şematik kesiti.

Depositional sequence 2

Underlying depositional sequence 1, a seismic unit with an oblique progradational pattern is identified as depositional sequence 2. The base and top of depositional sequence 2 are marked by apparent downlap and toplap of prograding clinoforms respectively (Fig. 15). The relative elevation of the topset to foreset transitions fluctuates (Fig. 15) suggesting parallel fluctuations in sea-level. The depositional sequence 2 blankets the floor of Izmir Bay, ranging in thickness from <10 ms to >100 ms. Depositional sequence 2 is divided into three

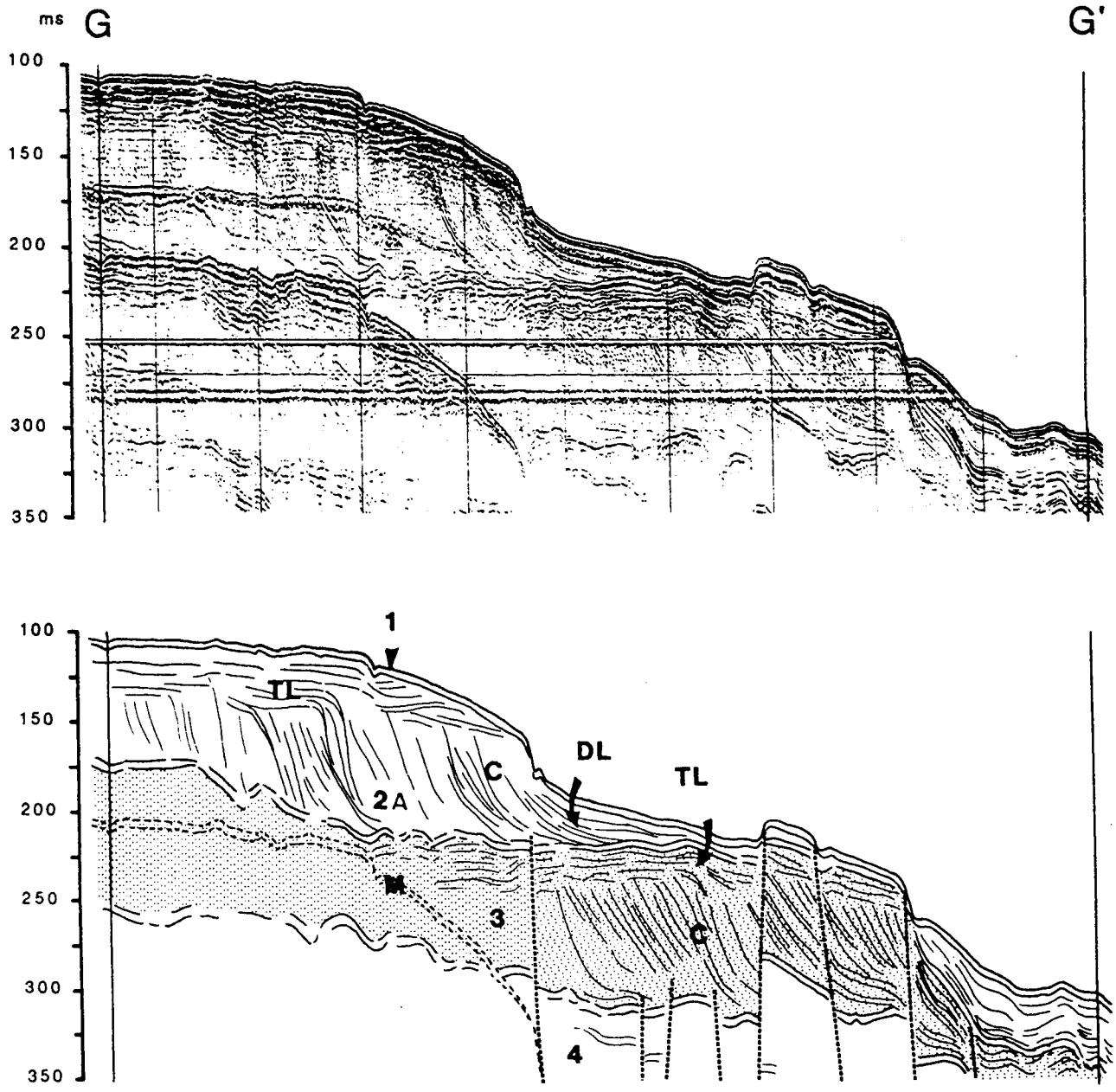

Fig. 15. Air-gun seismic profile (G-G') across the shelf break off Izmir Bay. Location is shown in Figure 2. 1 to 4 are depositional sequences; 2A is the depositional sequence related to the progradation of Gediz delta. TL= toplap, DL= downlap, C= clinoforms, M= multiple, dashed lines= faults. Profile is about 19 km long, vertical exaggeration= 39.

Şekil 15. Konumu Şekil 2'de görülen, İzmir Körfezi açığına ait hava tabancası sismik profili (G-G'). 1-4 depolanma istifleri olup, 2A Gediz Deltası ilerlemesiyle ilişkili bir depolanma istifidir. Burada TL= toplap, DL= downlap, C= klinoformlar, M= tekrarlı yansımalar kesikli çizgiler= faylardır. Profil uzunluğu 19 km ve düşey abartma 39'dur.

sub-units: 2A is related to the progradation of the Gediz delta and 2B and 2C are related to the progradation of the Bakırçay and Madra deltas, respectively (Figs. 16, 17). Figure 18 shows

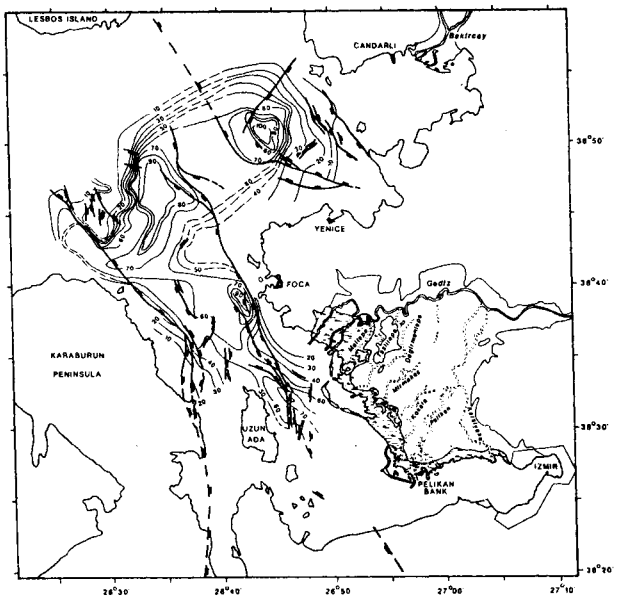

Fig. 16. Isopach map of Depositionalm Sequence 2 as related to sedimentation from Gediz river, showing sediment thickness in milliseconds two-way travel time. Heavy lines are faults with ticks on downthrown side. Acoustic source: air-gun.

Şekil 16. Gediz Nehri sedimentasyonuyla ilişkili 2 nolu depolanma istifi eşkalınlık haritası. Sediment kalınlığı milisaniye olarak gidiş-geliş zamanıdır. Faylar kalın çizgilerle işaretlenmiş olup, akustik kaynak hava tabancasıdır.

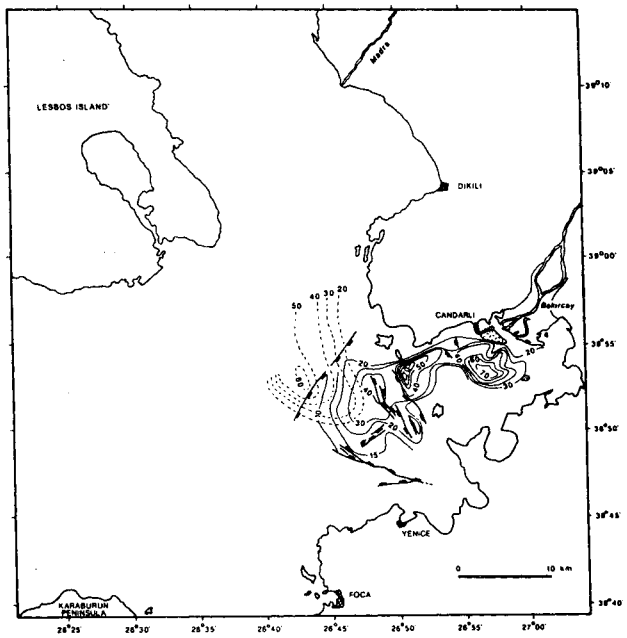

Fig. 17. Isopach map of Depositional Sequence 2 as related to sedimentation from Bakırçay (solid contours) and Madra (dashed contours) rivers, showing sediment thickness in milliseconds two-way travel time. Heavy lines are faults with ticks on downthrown side. Acoustic source: air-gun.

Şekil 17. Bakırçay (düz çizgiler) ve Madra Çayı (kesikli çizgiler) sedimentasyonlarıyla ilişkili 2 nolu depolanma istifi eşkalınlık haritası. Sediment kalınlığı milisaniye olarak gidiş-geliş zamanıdır. Faylar kalın çizgilerle işaretlenmiş olup akustik kaynak hava tabancasıdır.

that there are three major lobe development in sub-unit 2A. A large delta lobe is located immediately west of Foça (Fig. 16; lobe 1-2A in Fig. 18). It runs nearly parallel to the axis of Izmir Bay, and may represent a long duration delta encroachment during the gradually falling sea level of the last glacial. On the landward side of the modern shelf break in the approaches to Izmir Bay there is an elongate delta lobe that nearly parallels the present day bathymetric contours (Fig. 16; lobe 2-2A in Fig. 18). This large volume of sediment suggests a long duration for delta development in this area, fed by several distributaries. On the western side of Çandarlı Basin, depositional sequence 2A forms another, but smaller and confined delta lobe (Fig. 16; lobe 3-2A in Fig. 18). The geographic distribution and seismic character of this lobe suggest that it was developed by a single distributary, probably derived from the Pleistocene Gediz river.

On the eastern side of the Çandarlı Basin, depositional sequence 2B forms an other extensive delta lobe (Fig. 17; lobe 1-2B in Fig. 18). This large volume of sediment indicates a long duration delta development fed by the Bakırçay river. Data from the northern side of the Çandarlı Basin showed the progradation of a much smaller delta (Figs. 9, 17; lobe 1-2C in Fig. 18). The geographic distribution of this delta lobe suggests that it was fed by the Madra river. The distal deltaic sediments of the Gediz, Bakırçay and Madra deltas coalesce in the Çandarlı Basin.

Depositional sequence 3 and 4

Depositional sequences 3 and 4 are similar to deposi-

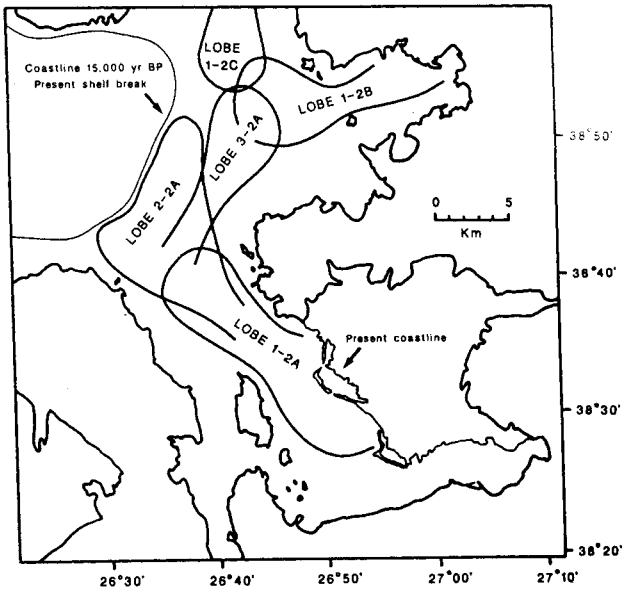

Fig. 18. Progradation of depositional sequence 2 of the Gediz, Bakırçay and Madra deltas during the last glacially lowered sea-level setting.

Şekil 18. Son buzul dönemine ait deniz seviyesi alçalımı sırasında Gediz, Bakırçay ve Madra Deltaları 2 nolu depolanma istifinin gelişimi.

tional sequence 2 in seismic character (Fig. 15), and represent earlier progradational deltaic deposits. They are best observed in the approaches to Izmir Bay, elsewhere in seismic profiles they occur below the maximum penetration of the acoustic source. Therefore, their distribution and thickness variations cannot be mapped.

(2) Büyük Menderes and Küçük Menderes seismic sequences

Four depositional sequences are identified in the Gulf of Kuşadası whereas only three depositional sequences occur in the Gulf of Güllük:

Depositional sequence 1

Depositional sequence 1 is a sigmoid progradational seismic unit composed of prograding clinoform reflectors (Figs. 10, 11), and it is seismically similar to the depositional sequence 1 observed in the Gediz and Bakırçay deltas. In the Büyük Menderes delta, the depositional sequence 1 forms a broad delta lobe that has prograded up to 5 km seaward of the modern coastline (Fig. 19). The prodelta platform is widest (3 km) and the depositional sequence 1 thickest (>80 ms) off the Karine lagoon, with steep prodelta slopes westward, where sequence 1 thins to less than 10 ms. The prodelta platform becomes narrow and the depositional sequence 1 thinner (<60 ms) to the south (Fig. 19).

Detailed analysis of 3.5 kHz profiles shows that three depositional sub-lobes can be recognised within the depositional sequence 1 of the Büyük Menderes delta (Figs. 20, 21). Isopachs on these units show that each represents a separate progradation at one point on the delta front, with corresponding erosion or slower deposition elsewhere. All three sub-lobes show sigmoid progradational seismic configuration, suggesting sedimentation during rising sea-level or rapid basin subsidence associated with slow sediment supply. These sigmoidal seismic reflectors are steepest and have the shallowest upper inflexion point off active river mouths. The oldest sub-lobe (1c) is restricted to the northern part of the delta off Karine lagoon (Fig. 20) and is related to the north Karine channel. The distribution and thickness of 1c suggests that the river discharge occurred north of the present distributary mouth, and the shoreline was probably at a position comparable to that of the present day. Sub-lobe 1b encircles the western periphery of an erosional platform off Karine lagoon (Figs. 20, 21), and it is related to deposition from the south Karine channel. The distribution and thickness of 1b suggest erosion near the platform (stipple in Fig. 20), and deposition of winnowed fines seaward, below the wave base. The occurrence of a relatively thick lobe immediately seaward of the present day mouth suggests that the Büyük Menderes channel was also active earlier. The youngest sub-lobe (1a) has three major sediment accumulations (Fig. 20) the oldest of which is confined to northwest Karine lagoon, suggesting deposition from north Karine channel. The southern accumulation encircles the Koca

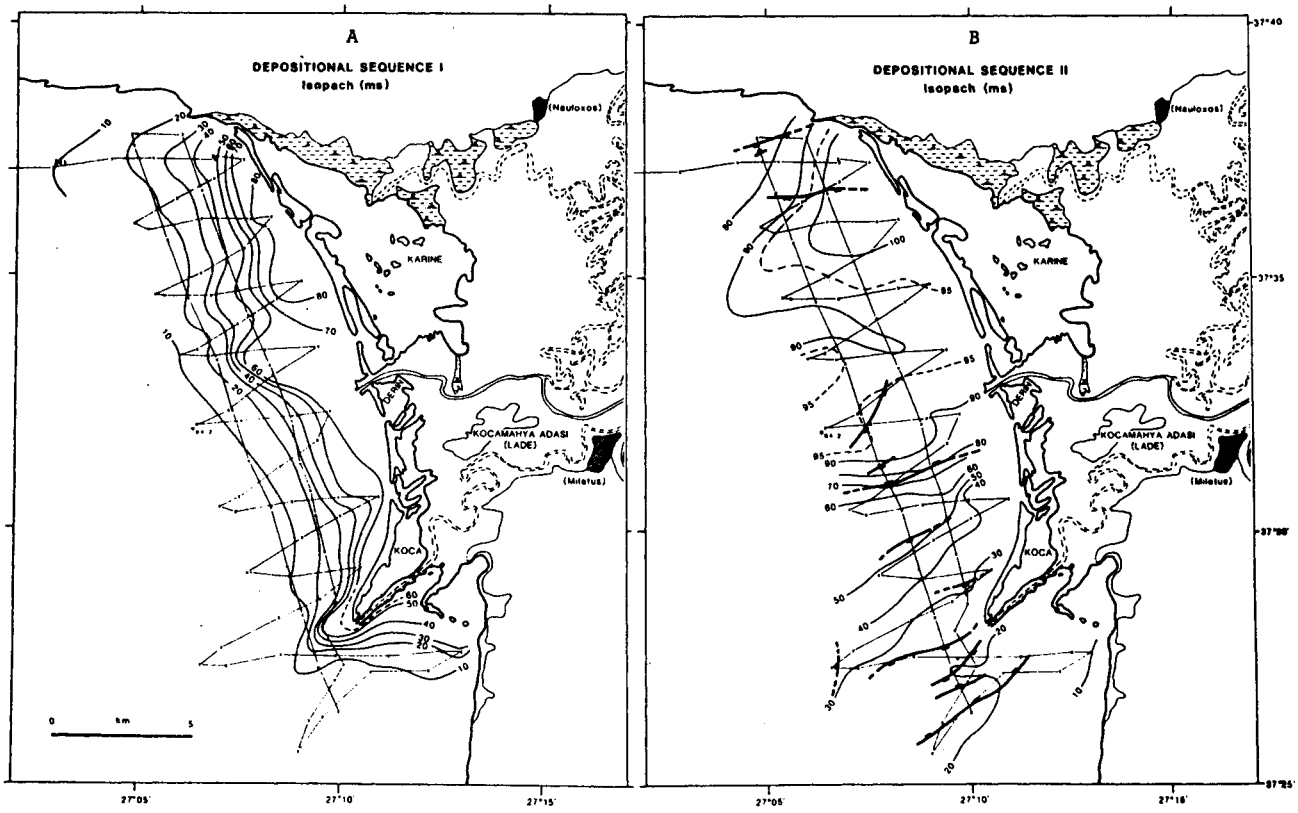

Fig. 19. Isopach maps of Depositional Sequence 1 and 2 in Büyük Menderes delta, showing sediment thickness in milliseconds two-way travel time. Heavy lines are faults with ticks on downthrown side. Acoustic source: air-gun.

Şekil 19. Büyük Menderes Deltası 1 ve 2 nolu depolanma istifleri eşkalınlık haritaları. Sediment kalınlıkları milisaniye olarak gidiş-geliş zamanıdır. Faylar kalın çizilerle işaretlenmiş olup, akustik kaynak hava tabancasıdır.

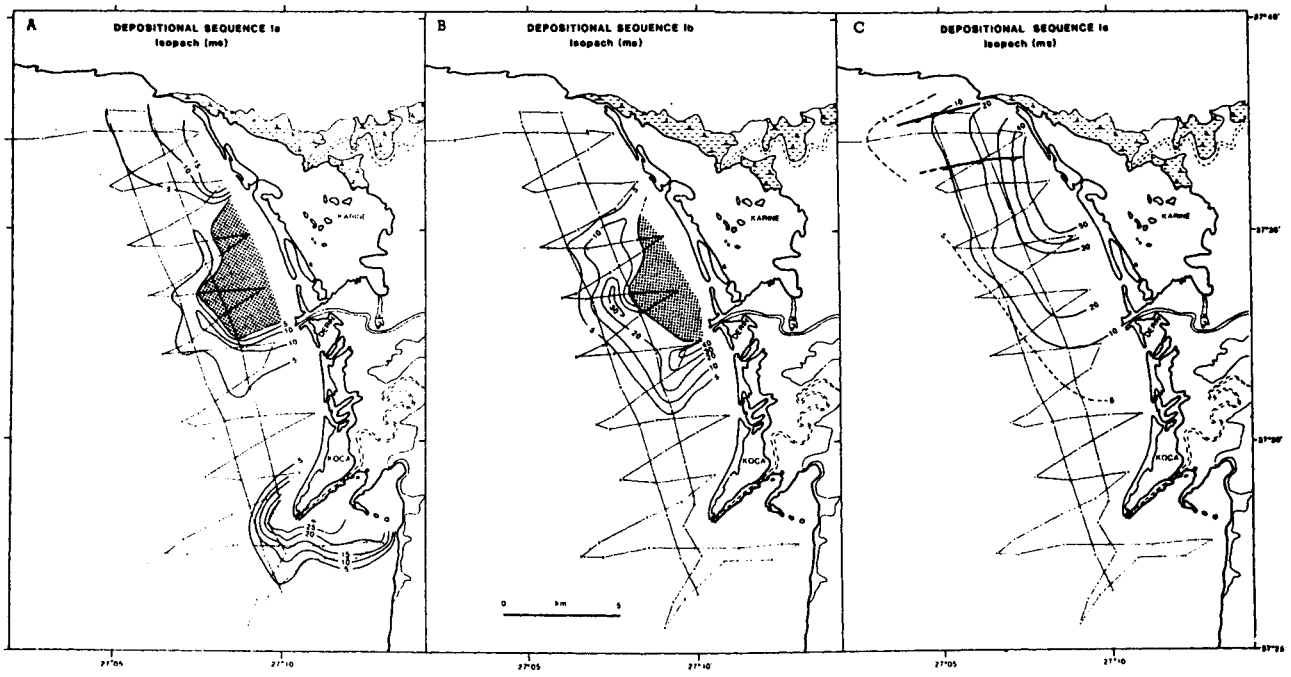

Fig. 20. Isopach maps of sub-lobes Ia to Ic in the Büyük Menderes delta showing sediment thickness in milliseconds two-way travel time. Heavy lines are faults with ticks on downthrown side. Acoustic source: 3.5 kHz. Shaded area= erosional platform, dashed lines= erosional contour.

Şekil 20. Büyük Menderes Deltası 1a-1c alt lobları eşkalanlık haritaları. Sediment kalınlıkları milisaniye olarak gidiş-geliş zamanıdır. Faylar kalın çizgilerle gösterilmiş olup, akustik kaynak 3.5 kHz'dir. Taralı alanlar erozyonal platformları, kesikli çizgiler aşınma hatlarını göstermektedir.

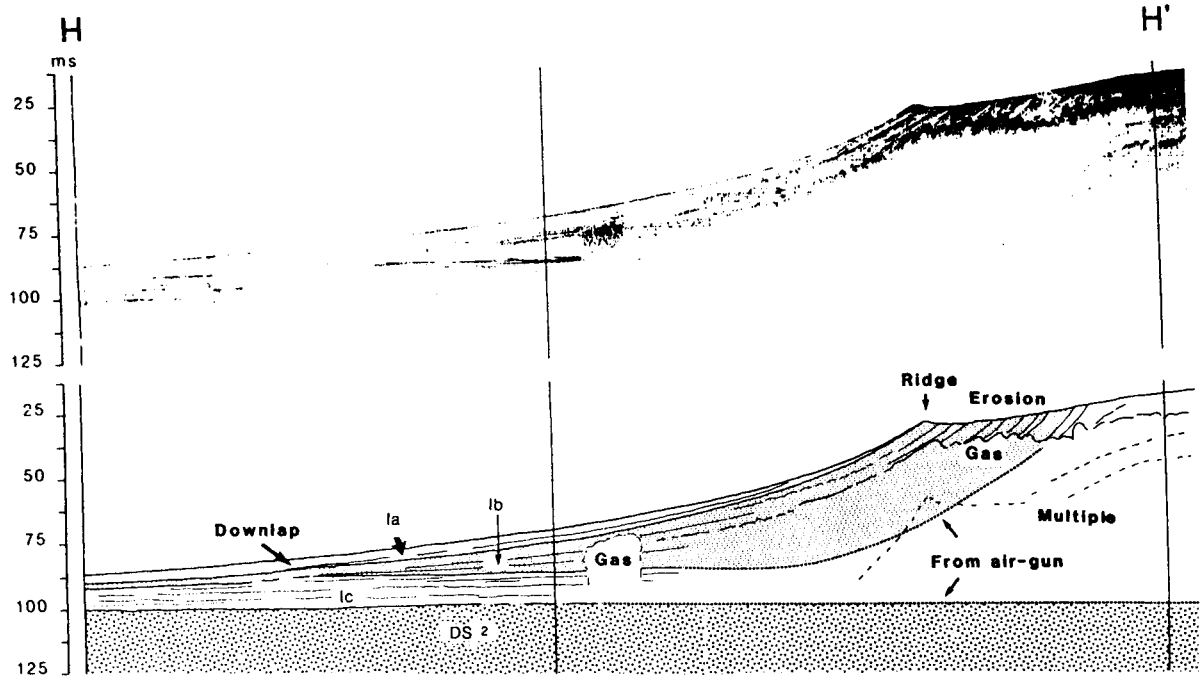

Fig. 21. 3.5 kHz seismic profile (H-H') from the Büyük Menderes delta. Location is shown in Fig. 3. 1a, 1b, 1c are sub-lobes of depositional sequence 1 discussed in text, DS 2= Depositional sequence 2. T= erosional truncation, B= ridge, DL= downlap, M= multiple. Section is about 4.5 km long, vertical exaggeration= 30.

Şekil 21. Konumu Şekil 3'de verilen Büyük Menderes Deltası 3.5 kHz sismik profili (H-H'). 1a, 1b, 1c; 1 nolu depolanma istifinin alt loblarıdır. DS2= 2 nolu depolanma istifi. T= erozyonal aşınma. B= Sırt, DL= downlap M= tekrarlı yansımalar. Profil uzunluğu 4.5 km ve düşey abartma 30'dur.

lagoon and is related to the Lade channel, thus may correspond to a phase of delta progradation in the Middle Ages that completely cut off sea travel to Miletus. The youngest sediment accumulation encircles the erosional platform (Fig. 20) and represents deposition from the Büyük Menderes channel before the Middle Ages as well as after 1945.

The successive sub-lobes indicate periodic shifting of the river mouth that can be broadly correlated with the progradation of the delta plain in historical times. Sub-lobe 1c probably correlates with the progradation of the northern delta plain until about 100 BC, and represents only the distal portion of this sub-lobe. The subsequent infilling of the southern half of the delta plain probably correllates with the growth of sub-lobe 1b. Sub-lobe la accumulated after the switch of channel in the Middle Ages from north of to south of Lade Island, and since that time wave erosion modified the proximal part of sub-lobe la.

The historical evidence suggests that the delta coastline prograded rapidly within the sheltered Büyük Menderes graben from 500 BC to 500 AD. There is no evidence for beach ridge formation during this time, and deposition was probably fluvially dominated with periodic channel avulsions. Barrier beaches formed once the river mouth prograded seaward of the protection of the Lade Island and the coastline to the south. This event is inferred to have occurred at about 700 AD. Since that time there has been only slow progradation of the coastline. Following each channel avulsion wave activity has modified the delta front and partially eroded the seaward edge of the abandoned lobes.

The 3.5 kHz profiles (Fig. 21) only penetrate to the base of depositional sequence 1 and show that this sigmoid wedge of sediment rests unconformably on a irregular accoustic basement. This basement probably was the subaerially exposed delta flood plain during the peak of the last major lowering of sea-level, some 20,000 yr BP.

The Holocene Küçük Menderes delta is similar to that of Büyük Menderes, except that only a single depositional lobe can be distinguished (Fig. 22). This is a result of the much greater constriction of the delta plain by bedrock near the coastline. The Küçük Menderes delta shows a similar history of progradation, with rapid westward fluvially dominated growth from 900 BC to 300 AD, followed by development of a wave-dominated delta coastline once the river mouth entered the Gulf of Kuşadası. Depositional sequence 1 progrades over depositional sequence 2 and it is apparently very thin or absent west of the 60 m bathymetric contour (Figs. 7, 22).

Depositional sequence 2

The data from the Büyük Menderes covers only a narrow strip of the Pleistocene delta close to the present shoreline. Delta sedimentation has been concentrated is the northern part of Gulf of Güllük, suggesting that the river discharged north of the Lade Island (Figs. 11, 19).

Depositional sequence 2 in the Küçük Menderes delta is an oblique progradational seismic unit where clinoforms terminate updip by toplap near a horizontal reflector and downlap against the older, near-horizontal reflectors. Three delta progradation lobes are observed in depositional sequence 2. Lobe 2C underlies the younger lobes (Fig. 7) and prograded about 10 km west of the modern coastline into the Gulf of Kuşadası (Fig. 23). The seaward limit of lobe 2C is marked by an irregular gentle slope similar in profile to that seen of inactive portions of Holocene delta. It is directly overlain by steep prograding clinoforms of lobe 2B and 2A indicative of renewed progradation near the river mouth. Lobe 2B prograded southwestward, and lobe 2A northwestward to build the modern shelf edge. Immediately seaward of the limit in lobe 2C in

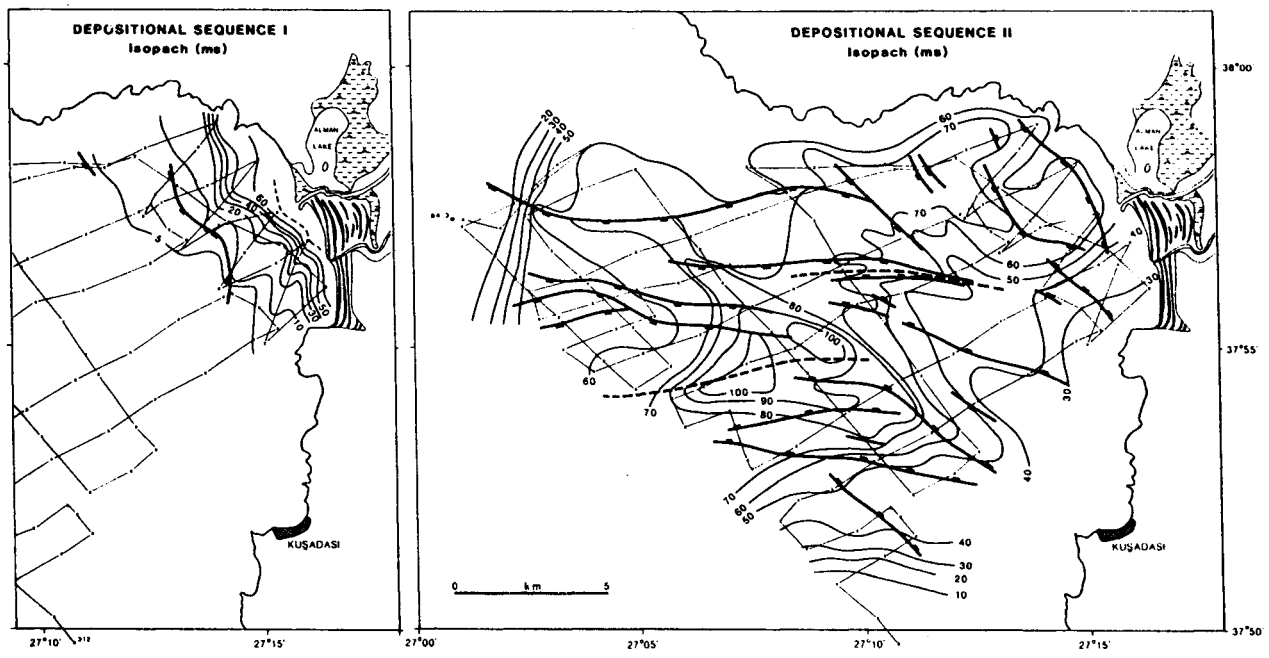

Fig. 22. Isopach maps of depositional sequence 1 and 2 in Küçük Menderes delta showing sediment thickness in milliseconds two-way travel time. Heavy lines are faults with ticks on downthrown side. Acoustic source: air-gun.

Şekil 22. Küçük Menderes Deltasına ait 1 ve 2 nolu depolanma istifi eşkalınlık haritaları. Sediment kalınlıkları milisaniye olarak gidiş-geliş zamanıdır. Faylar kalın çizgilerle işaretlenmiş olup, akustik kaynak hava tabancasıdır.

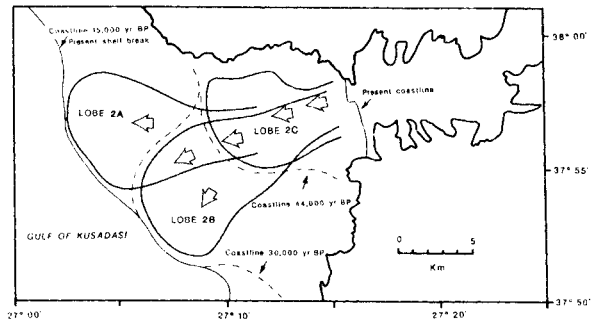

Fig. 23. Progradation of depositional sequence 2 of the Küçük Menderes delta during the last glacially lowered sea-level setting. Arrows indicate depositional mouth (discussed in text), dashed lines indicate palaeocoastline.

Şekil 23. Son buzul dönemine ait deniz seviyesi alçalımı sırasında Küçük Menderes Deltası 2 nolu depolanma istifinin gelişimi. Oklar depolanma ağzını (metinde tartışılan), kesik çizgiler eski kıyı hattını göstermektedir.

Figure 7, the upper inflexion point in sigmoid prograding clinoforms in the lower part of lobe 2A becomes progressively higher (x in Fig. 7), suggesting coastline stability and upward growth of a barrier complex during a phase of relative rise in sea-level (which may result from delta subsidence during stable eustatic sea-level). The apparent angle of dip of clinoforms in lobe 2A may vary due to proximity to a river mouth and to the angle between the seismic line and the depositional strike. The variation in these dips suggests that the lobe prograded in a number sub-lobes with dimensions similar to those observed in the Holocene büyük Menderes delta.

Detailed examination of the seismic data shows no evidence for buried distributary channels. However, the relative position of the distributary mouth could be determined from the direction of foreset progradation. This is best observed in strike sections and characterized by symmetrical prograding clinoform pattern in which a number of relatively steep-dipping reflectors diverge from a point (illustrated in the Büyük Menderes as DM in Fig. 11). The inferred positions of distributary mouths in depositional sequence 2 of the Küçük Menderes delta are shown in Figure 23.

In places between the shelf break and the shoreline, the uppermost part of depositional sequence 2 includes lenticular seismic units that are shingled one on top of the other. Internally they exhibit weak to moderate, horizontal to shingled reflectors that downlap the lower surface of the units. These shingled units become thicker but less extensive landward, and are interpreted as transgressive deltaic and marine deposits that progressively onlap the ancestral coast during Holocene sea-level rise. In places, these shingled units have a distinct surface relief which are interpreted as relict coastal barriers. On several seismic lines seaward of the 70 m isobath there are small sediment ridges at about 110 m isobath (y on Fig. 7) that may represent old barrier ridges.

Depositional sequence 3 and 4

Depositional sequences 3 and 4 are similar in seismic character to depositional sequence 2, and probably represents earlier delta progradation during lower sea-level stands (Fig. 7). It is best represented off the Küçük Menderes delta, but elsewhere in the seismic profiles they occur below the resolution of the data.

INTERPRETATION OF DEPOSITIONAL SEQUENCES

Depositional sequence 1 is the result of Holocene delta progradation during the most recent high stand of sea level. It is separated from depositional sequence 2 by a major transgressive surface on which only thin transgressive sediments have accumulated. The depositional sequence 2 represents a major advance of delta progradation during the last major low stand of sea level some 20,000 years ago (Aksu and Piper 1983, Aksu *et al.* 1987a, b). The underlying depositional sequences 3 and 4 represent analogous phases of delta progradation; the prominent transgressive surfaces that separate depositional sequences 2, 3, and 4 represent major marine transgression similar to that in the Holocene.

CORE DATA

(1) Lithofacies

Based on colour, grain size and mineralogical analyses the sediments recovered in the cores are divided into four lithofacies:

Facies A consists of light brown, moderately sorted, medium grained sands with abundant broken shell fragments and usually less than 3% gravel (Figs. 24, 25). About 80% of

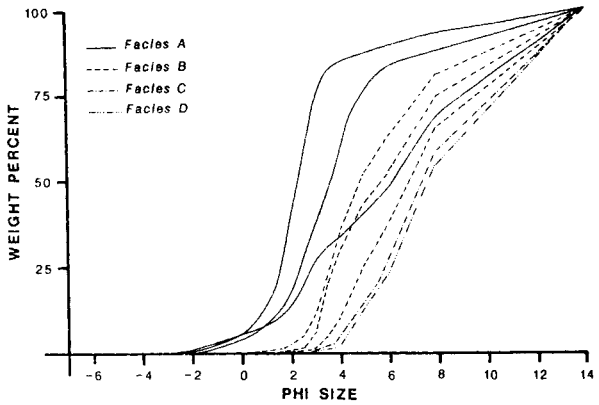

Fig. 24. Grain size plots of different facies in cores recovered from the outer Izmir and Çandarlı Bays.

Şekil 24. Dış İzmir ve Çandarlı Körfezlerinden alınan karotlarda farklı fasiyeslere ait tane boyu dağılım grafikleri.

the sand-size clasts consist of biogenic carbonate debris, mostly foraminifera and mollusc shells. X-radiographs show no apparent stratification. This facies forms a 15-50 cm thick veneer at the uppermost portion of cores from the outer Izmir Bay and Gulf of Kuşadası. It is also found below the surface clayey muds (facies C) around the periphery of the Çandarlı Basin (Fig. 25) as well as underlying the prodelta sand/silt to mud couplet (facies B) in the outer Izmir Bay. Facies A correlates with the uppermost part of the seismic depositional sequence 2 in the outer Izmir Bay and Gulf of Kuşadası and interpreted to represent the topset beds of the last glacial delta.

Facies B consists of olive grey/green mud with frequent silt/sand laminations, 0.2-1.0 cm thick and occurs immediately below Facies A (Figs. 24, 25). Sediments in this facies are heavily bioturbated. Occasionally, lenticular lamination is visible on X-radiographs. The upper and lower contacts of the laminae are often gradational and disturbed and the silt/sand laminae are mixed with the overlying and underlying sediments. Rare shell fragments also occur in this facies. Facies B

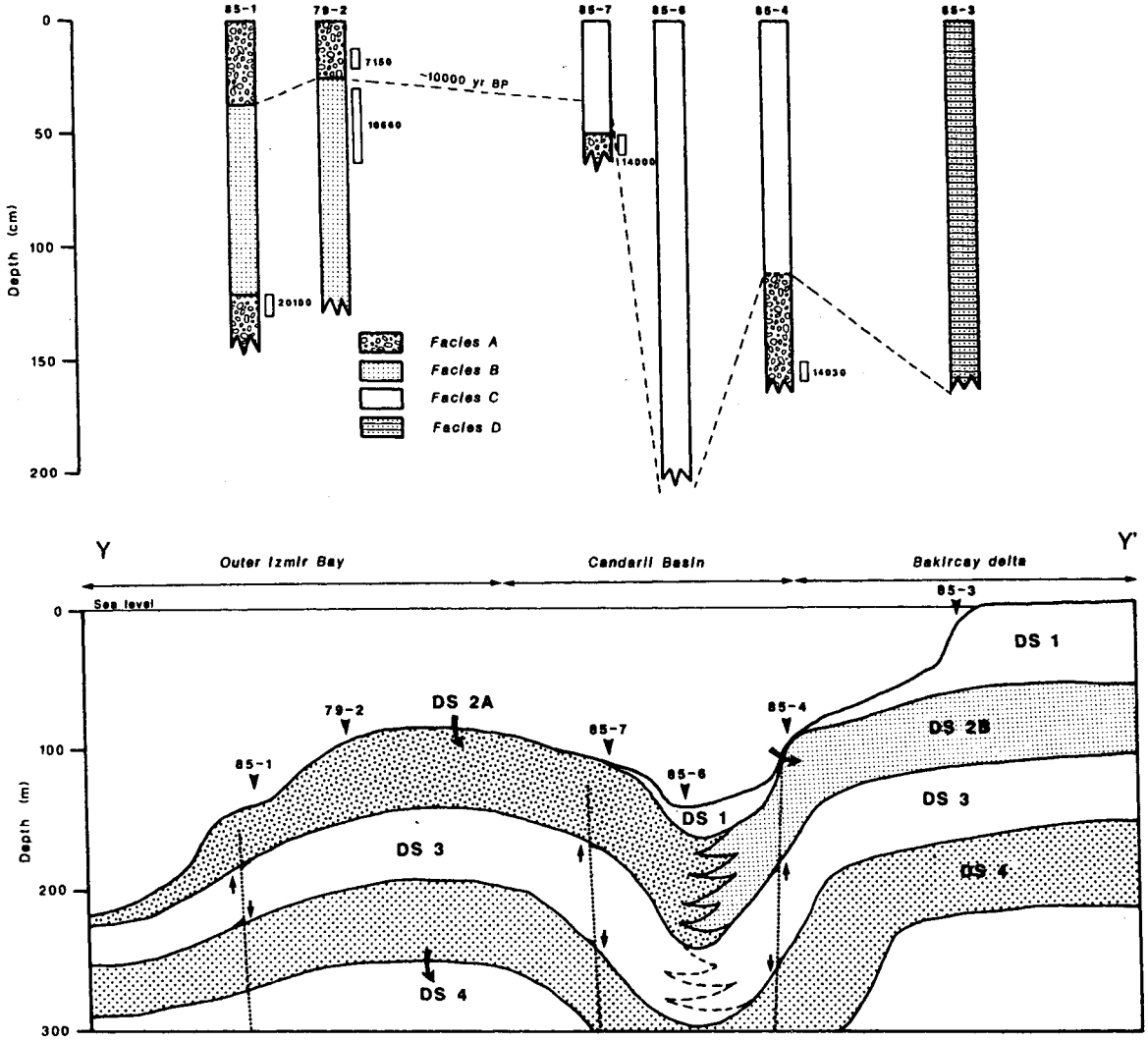

Fig. 25. Detailed core logs, lithofacies distribution and correlation of cores recovered from the outer Izmir and Çandarlı Bays (Top). Schematic geological cross section Y-Y' showing the relationship of the physiography and the lithofacies recovered in the cores (Bottom). Location in Fig. 2.

Şekil 25. Dış İzmir ve Çandarlı körfezlerinden alınan karotların litofasiyes dağılımı ve ilişkileri ile ayrıntılı logları (üst şekil). Konumları Şekil 2'de verilen karotlarda litofasiyesler ve fizyografik ilişkileri gösteren Y-Y' şematik jeolojik kesiti (alt şekil).

is correlated with the clinoforms of the seismic depositional sequence 2 in the outer Izmir Bay and the Gulf of Kuşadası. It is interpreted to represent the prodelta facies of the last glacial delta.

Facies C consists of olive grey/green fine clayey mud with usually less than 5% sand and silt. The coarse fraction is almost entirely composed of biogenic carbonate debris. X-radiographs show this facies to be moderately bioturbated with no apparent stratification. Rarely very faint horizontal fine silt laminations are also observed on the X-radiographs. Facies C occurs only in the Çandarlı Basin and is interpreted as hemipelagic sedimentation in an isolated basin augmented by occasional density flow deposits entering into the basin from the east, associated with heavy discharge patterns of the Bakırçay river (Figs. 24, 25).

Facies D consists of olive grey/green muds with occasional sand/silt to mud couplets (Figs. 24, 25). The coarse fraction in this facies includes higher percentages of sand/silt-size terrigenous clastics than that observed in facies C and the sediments are extensively bioturbated. Facies D occurs immediately seaward of the present-day river mouths and probably represent present-day prodelta sedimentation.

(2) Micropaleontology

Three cores were sampled for micropaleontological studies. Core 84-3 was collected from the prodelta slope of lobe 2A, off the Pleistocene Küçük Menderes delta (Fig. 4). The core penetrated a thin veneer of sandy mud (facies A) over mud with frequent silt laminae (facies B). Core 85-1 was taken from the bottomset zone of the Pleistocene Gediz delta (Fig. 2). The core penetrated a 37 cm thick veneer of muddy sand with abundant shell fragments (facies A) and recovered about 63 cm of mud with silt laminae (facies B). Underlying the silts and muds, the core also penetrated a 50 cm thick muddy sand similar to that recovered at surface (facies A). Core 79-2 was also collected from the upper foreset zone of the Pleistocene delta in the outer Izmir Bay. The core penetrat-

ed a 25 cm of sands with abundant broken shell fragments (facies A) and recovered about 100 cm of sand/silt to mud couplets (facies B).

The surface muddy sands (facies A) included a rich and diverse benthic and planktonic fauna and flora (Fig. 26). The planktonic foraminiferal assemblage is dominated by *Globigerinoides ruber, Gs. conglobatus, Gs. sacculifer* with smaller percentages of *Orbulina universa, Globigerinella aquilateralis, Globorotalia crassaformis* and *Globigerinita glutinata*. The benthic foraminiferal assemblage is dominated by *Textularia pseudorugosa, T. ponderosa, Planulina wuellerstorfi, Rosalina colombiensis, Cassidulina reniforme, C. laevigata*. These sediments also include high coccolith abundances dominated by *Emiliania huxleyi* var. warm with lesser quantities of *Cyclococcolithina leptopora, Gephyrocapsa oceanica* and *Helicopontosphera kamptneri*. These benthic and planktonic foraminiferal and coccolith assemblages are consistent with the present-day water depth, temperature and salinity characteristics of the eastern Aegean Sea (Thunell 1978, Aksu and Piper 1983).

The underlying muds with silt laminae (facies B) included a sparce and low diversity planktonic and benthic foraminiferal fauna (Fig. 26). The planktonics are dominated by *Neogloboquadrina pachyderma* dextral, *Globigerina bulloides, G. quinqueloba* and *Gs. ruber*. The benthics are dominated by *Ammonia beccarii, Elphidium crispum, Haynesina depressulum, Cribrononion excavatum, C. excavatum lideonsis* and *Quinqueloculina seminulum*. This benthic and planktonic foraminiferal fauna is similar to those described by Aksu and Piper (1983) and represents a coastal brackish environment with water depth not exceeding 30 m. The coccoliths abundances are extremely low in this lithology, suggesting either very low coccolith production due to shallow water depth and lowered salinity or major dilution by terrigenous detritus. The abrupt change from brackish, shallow water to normal salinity shelf benthic fauna associated with the change from cool to subtropical planktonic fauna is probably the result of both rising sea level and warming of sea water temperature and probably represents a change from glacial to Holocene sediments.

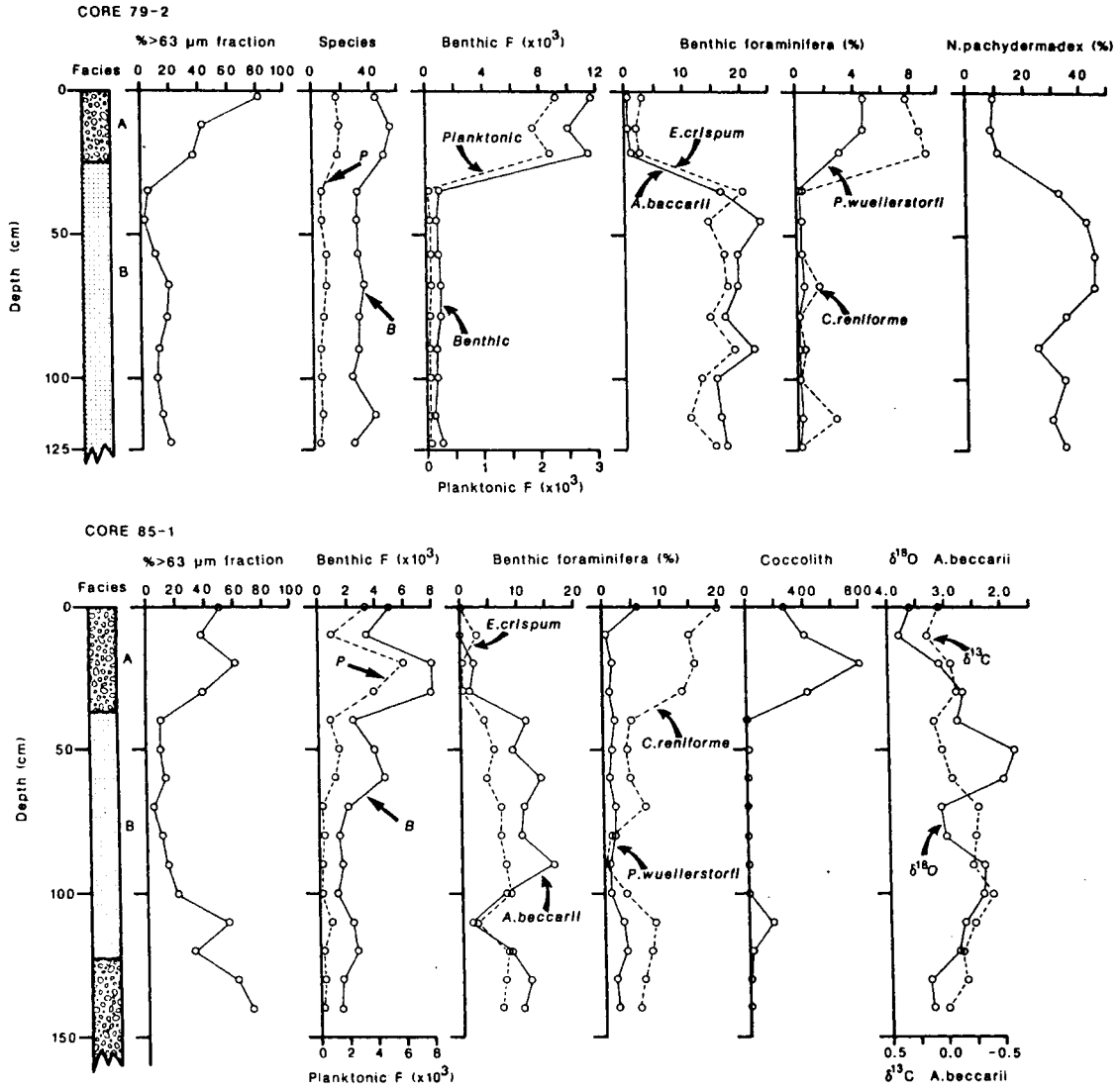

Fig. 26. Rediocarbon dates in yr BP, lithofacies, geochemical and micropaleontological data in cores 79-2 and 85-1.

Şekil 26. 79-2 ve 85-1 nolu karotlardan alınan, yılda BP olarak saptanan radyo karbon tarihleri ile litofasiyes, jeokimyasal ve mikropaleontolojik veriler.

The lowermost muddy sands (facies A) in core 85-1 included planktonic and benthic foraminiferal and coccolith abundances and assemblages similar to those found in the muds with silt laminae (Fig. 26). These data suggest coastal brackish to marine conditions at the core site.

(3) Stable isotopes

Oxygen and carbon isotopic compositions of benthic foraminifera *A. beccarii* were determined in core 85-1 using a VG MM 903 mass spectrometer (Fig. 26). The $\delta^{18}0$ values of the upper ca. 37 cm in the core (facies A) varied from 3.0 to 3.8‰. Foraminifera from the underlying facies B and the deeper facies A yielded oxygen isotopic values ranging from 1.6 to 3.0‰, averaging 2.5‰. In marginal seas and coastal environments, the use of the oxygen isotopes as a chronostratigraphic tool becomes questionable. In these environments the $\delta^{18}0$ values of foraminifera primarily reflect the changes in the $\delta^{18}0$ composition of the sea water in which foraminifera lived. In tern, the $\delta^{18}0$ composition of the sea water is a function of its salinity.

Deep-sea oxygen isotopic data from the eastern Mediterranean (eg. core RC9-181; Fig. 27) shows that during interglacial periods the $\delta^{18}0$ composition of planktonic foraminifera *G. ruber* varied from 0.0 to -2.0‰; with glacial values averaging around 1.0 to 2.0‰. Because the species dependent fractination of *A. beccarii* is not known, estimates of the geographic variation in the $\delta^{18}0$ composition of the sea water during glacial and interglacial periods cannot be made. Deep-sea record, however, clearly shows that the interglacial $\delta^{18}0$ values are much lighter than those in the glacial periods. Comparison of the $\delta^{18}0$ records of the deep-sea Mediterranean and core 85-1 (Figs. 26, 27) shows that the oxygen isotopic composition in core 85-1 is a mirror image of core RC9-181, with interglacial $\delta^{18}0$ values being much heavier than those of glacials. The heavier $\delta^{18}0$ values in the surface facies A probably represent normal marine shelf conditions; whereas, the observed 1.0 to 1.5‰ depletion in the $\delta^{18}0$ in facies B represents considerable reduction in the salinity of the sea water at the core site during the deposition of facies B. The oxygen isotopic data independently confirms the presence of brackish water conditions during the deposition of facies B suggested by the micropaleontological data. The carbon isotopic data shows similar but much attenuated variations.

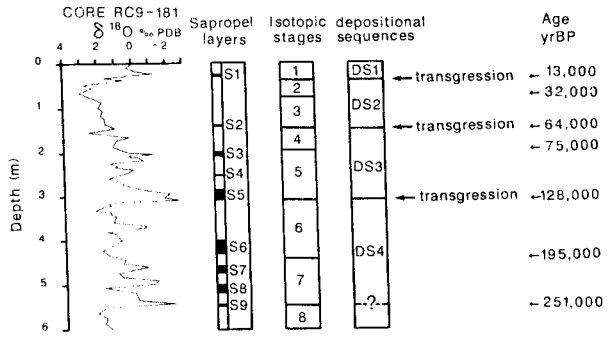

Fig. 27. Oxygen isotopic variations in planktonic foraminifera *(Globigerinoides ruber)* in core RC9-181 (33°25'N, 25°01'E, 2286 m) showing the paleoclimatic record of the eastern Mediterranean Sea (from Vergnaud-Grazzini et al. 1977), sapropel layers (from Cita et al 1977), sapropel layers (from Cita et al. 1977), ages of isotopic stage boundaries from Shackleton and Opdyke (1976).

Şekil 27. RC9-181 (33°25'N, 25°01'E, 2286 m) nolu karotta planktonik foraminifer *(Globigerinoides ruber)* de oksijen izotopu değişimleri; doğu Akdeniz'in paleoklimatik kayıtlarıyla ilgili bu veriler Vergnaud-Grazzini ve diğ. 1977, sapropel katmanları Cita ve diğ. 1977, izotopik dönem değişim tarihleri de Shackleton ve Opdyke 1976 dan alınmıştır.

(4) Carbon-14 dates

A total of five ^{14}C dated were obtained from 4 cores (Table 2). Mollusc and foraminiferal carbonates from the basal 10 cm of facies A in core 79-2 yielded a data of 7,150 yr BP. A total organic carbon date of 10,660 yr BP was obtained from the to 20 cm of the facies B in core 79-2. The uppermost 10 cm of the facies A in core 85-7 in the Çandarlı Basin yielded an age of 14,000; similarly the base of core 85-4 (facies A) is dated as 14,030 yr BP. The uppermost 10 cm of the facies A underlying the prodelta muds of facies B in core 85-1 gave an age of 20,100 yr BP.

(5) Mineralogy and grain size

X-ray diffraction analyses of the <2μm fraction in core 79-2 shows that the principal clay minerals are montmorillonite, illite and kaolinite. No significant differences between the Holocene and Pleistocene sediments were distinguished. Heavy mineral analysis was carried out on the 3-4 Φ size fraction of twelve samples from core 79-2 (Table 3). Heavy mineral abundances are generally between 1 and 4%, but reached 15 and 23% in two samples. The heavy mineral assemblage is dominated by opaque minerals, garnet and amphibole, with lesser amounts of apatite and pyroxene. Opaque minerals are

CHRONOLOGY OF DEPOSITIONAL SEQUENCES

In outer Izmir Bay and Gulf of Kuşadası the shelf break denotes the topset to foreset transition of the last stage of delta progradation during the last glacial period (isotopic stage 2) prior to post-glacial sea level rise (Aksu and Piper 1983). Mi-

Table 2. Carbon-14 dates obtained in cores used for this study. TAM= Tanum accelerator mass spectrometry dates

Çizelge 2. Bu çalışmada kullanılan orlarda karotlarda tesbit edilen Karbon-14 tarihleri. TAM ise "Tanum Accelerator Mass" spektromete tarihleridir

CORE	DEPTH (CM)	^{14}C DATES YR BP	LABORATORY	LAB. NO.	MATERIAL DATED
79-2	12-22	7150 ± 110	Beta Analytical	Beta 6281	shell
79-2	30-63	10660 ± 810	Beta Analytical	Beta 6282	organic carbon
85-1	120-130	20100 ± 420	Beta Analytical	Beta 15248	TAM shell
85-4	150-159	14030 ± 260	Beta Analytical	Beta 15246	TAM shell
85-7	50-59	1400 ± 240	Beta Analytical	Beta 15247	TAM shell

Table 3. **Heavy mineral and grain size distribution in two cores from the outer Izmir Bay. Heavy mineral data exclude micas. Sample preparation and heavy mineral identifications are made following the technique described in Aksu (1981).**

Çizelge 3. **İzmir Körfezi dışında alınan iki karotta ağır mineral ve tane boyu dağılımı. Mikalar bu verilere dahil edilmemiştir. Örnekleme ve ağır mineral tayinleri Aksu (1981)'de ayrıntılı olarak açıklanan teknikler kullanılarak yapılmıştır.**

	Core 79-5						Core 79-2					
Depth (cm) →	0	21	45	70	100	125	0	25	50	75	100	120
Minerals (%) ↓												
O. pyroxene	7	7	1	2	1	4	9	12	8	5	7	8
C. pyroxene	12	8	2	1	1	2	16	5	6	8	9	8
Opaques	19	38	74	74	73	70	8	7	17	33	11	7
Altered	6	3	18	18	19	9	2	4	9	6	8	6
Tourmaline	5	1	1	0	0	1	5	7	3	2	7	5
Zircon	0	0	0	0	0	0	1	0	0	0	0	0
Garnet	23	6	1	2	1	8	37	29	32	26	33	31
Apatite	5	6	1	0	2	2	4	9	7	6	8	6
Amphibole	19	29	2	3	2	5	17	24	16	13	15	27
% heavy	3.6	1.4	15.0	23.0	7.4	3.2	1.4	1.7	4.0	2.8	2.2	2.3
grain size ↓												
% gravel	2.3	0.0	0.0	0.0	0.0	0.0	2.4	0.5	0.0	0.0	0.0	0.2
% sand	31.2	42.6	2.3	2.8	29.7	29.7	82.2	35.2	22.9	31.9	24.0	35.0
% silt	35.8	34.8	52.2	56.3	45.1	45.1	8.2	47.7	54.0	49.9	53.9	46.1
% clay	30.7	22.6	45.5	41.0	25.2	25.2	7.2	16.7	23.1	18.1	22.1	18.8

cropaleontological data from two gravity cores which penetrated the upper part of depositional sequence 2 indicated that these sediments were deposited in a brackish, shallow water environment. Radiocarbon dates from the top of the foresets in depositional sequence 2 suggested that foreset progradation in the area ceased between 14,000 and 10,000 yr BP. There has been little sedimentation since that time and outer Izmir Bay is floored by relict shoreface sands (Aksu and Piper, 1983).

During the Quaternary period, there have been episodes of stagnation in the eastern Mediterranean Sea producing distinctive and correlatable sapropel layers. Several theories have been proposed for the association of sapropel deposition and global climatic fluctuations. Thunell *et al.* (1977) and Vergnaud-Grazzini *et al.* (1977) indicated that sapropels were developed when rising sea-level re-established the communication between the mediterranean Sea and the Black Sea allowing an influx of glacial meltwater augmented by increased pluvial conditions during the transition from glacial to interglacial conditions.

There are five well defined sapropel layers within the last ca. 150,000 yr record (Cita *et al.* 1977): S1 corresponds to the Holocene transgression (isotopic stage 2/1). S2 corresponds to the transgression at the isotopic stage 4/3 boundary, and S3, S4, and S5 occur at the beginning, middle, and end of isotopic stage 5 (Fig. 27). Uranium-series dating of marine fossils from raised beach terraces around the Mediterranean has indicated high stands of sea level (i.e. comparable to that of present day) during isotopic stages 1 and 5 (Stearns and Thurber 1965), and the occurrence of sapropel layer S2 requires a sea-level rise to at least - 40 m (minimum depth of the Bosphorus sill).

Low stand of sea level (-110 m) during the last glacial period is suggested by Stanley and Blanpied (1980) and Aksu and Piper (1983). The oxygen isotopic records of a number of cores from the eastern Mediterranean Sea also suggested low stands of sea level during glacial isotopic stages 2, 4, 6, and 8 (Vergnaud-Grazzini *et al.* 1977).

Both the sapropel horizons and the major transgressive surfaces between the stacked prograding delta sequences mark periods of rapid sea level rise, although there may not be a one-to-one correlation. Sapropel S1 clearly correlates with the 2/1 transgression (Figs. 27, 28). Two methods are available to estimate the age of the other transgressive surfaces: examination of fault offsets and consideration of total sediment volumes in the progradational sequences.

Fault offsets (discussed later) indicate that the 3/2 transgressive surface is about 5 times older than the 2/1 surface, suggesting an age of some 55,000 years for this surface. This most reasonably correlates with the S2 sapropel at the base of isotopic stage 3, with an age of about 60,000 years. We have little data on fault offsets that cut both the 3/2 and 4/3 transgressions: the limited data suggest that the 4/3 transgression is at least twice as old as the 3/2 and therefore most reasonably corresponds to sapropel S5 in isotopic stage 5e, which was a time when sea levels globally were a little higher than at present.

The total sediment volume associated with depositional sequence 3, to within the limits of our data coverage, appears similar to that in depositional sequence 2. If the sedimentation rates are comparable during these periods, this would suggest that the two sequences were of approximately similar duration. Furthermore, the total volume of sediments in the depositional sequence 2 in the outer Izmir Bay is estimated at 65 km^3 (Fig. 16). There may be a similar volume of sediment of this age trapped within the inner parts of Izmir Bay and the modern areas of the Gediz delta. Modern sediment discharge of the Gediz river is of the order of 5 km^3 per thousand years. If glacial sediment discharge was at a similar rate and all sediments was trapped within the delta, this suggests that depositional sequence 2 is of 20 to 30 thousand years duration. This

is broadly consistent with the chronology suggested by the fault offsets and the micropaleontological data.

A DELTA PROGRADATION MODEL

In the late Quaternary there has been an alternation of periods of marine transgression with periods of regression, with only short times of stillstand. Many of the transgressions have been rapid, whereas most regressions have been slower. High stands of sea level, corresponding to residual ice only in Antarctica and Greenland, occur at the present time, and also occured in isotopic stage 5e, and during some earlier interglacials.

(1) Gediz, Bakırçay and Madra

In the present-day Gediz and Bakırçay deltas (depositional sequence 1) the topset to foreset transition occurs around 20 msec (15 m) water depth. An analogous transition occurs at about 150 msec (112.5 m) water depth in depositional sequence 2 of both the Gediz and Bakırçay deltas. The topset to foreset transition in depositional sequence 3 occurs around 225 msec, 75 msec below the transition in depositional sequence 2A. The topset beds of depositional sequence 4 are located about 90 msec below the foreset beds of depositional sequence 3. If the topset to foreset transitions of each delta occurred at around 15 m water depth, and if the extent of sea level lowering during delta progradation is known, the amount of subsidence can be calculated. On the basis of oxygen isotopic records from the world ocean, it appears that the global ice volume at the peak of isotopic stage 2 and at the peak of isotopic stages 4 and 6 were similar (Shackleton and Opdyke 1976), suggesting that the "eustatic" sea-level lowering was of similar magnitude. It is, therefore, assume that the topset to foreset transition at the top of depositional sequences 2, 3 and 4 developed under conditions of similar lowering of sea level. The difference in elevation between depositional sequences 2 and 4 averages 132 m. Errors in relating this transition to true sea level must be equal at both stratigraphic levels and, therefore, cancel out; errors associated with assuming similar low stand of sea level is probably no more 15 m. We use 115,000 years as the estimate of the time from the peak of stage 6 to the peak of stage 2. This implies a subsidence rate of 1.15 m per thousand years at the southeastern margin of the Karaburun Basin. The tectonic subsidence calculated here compares favorably with 1-2 m/1000 years suggested by Flemming (1972).

Depositional sequences 2 and 1 illustrate a complete depositional cycle from slow regression through rapid transgression to the modern stillstand of sea level. From the evidence of topset to foreset transition elevations, it is suggested that the depositional sequence 2 developed by delta progradation during a low stand of sea level. During much of this time, sea level was falling slowly, allowing the delta to build forward into deep water. The lowest position of the topset to foreset transition corresponds to the maximum fall of sea level in isotopic stage 2, estimated at -100 to -115 m (Aksu and Piper 1983) in this area. The rapid transgression around the isotopic stage 2/1 transition resulted in deposition of a thin transgressive sediment sheet and the retreat of the deltas far up long coastal bays (Aksu and Piper 1983). Since sea level stabilised about 5000 years ago, the inner parts of these bays have been filled in and the deltas are prograding seaward in equilibrium with modern sea level. With a gradual lowering of sea level, the deltas would continue to prograde seaward. The gradient of the continental shelf is such that a gradual lowering of sea level would not significantly steepen river thalweg (Fig. 5).

The age of the delta lobes within the depositional sequence 2 has been estimated on the basis of their total volume and the modern discharge rates of the Gediz river. Lobe 1-2A prograded from the headland of the ancestral bay to a line joining Foça and Karaburun and reached its maximum extent at about 35 000 BP (Fig. 18). At this point Izmir Bay widens rapidly, and opens to an area with much longer wave fetch. The sudden widening of the bay and the increased wave activity probably caused the halting of delta advance. Therefore this period may represent a transitional stage from predominantly fluvially dominated delta to wave dominated Gediz delta. With continued lowering of the sea-level, lobe 2-2A prograded northwestward into the Karaburun Basin (Fig. 18). At about the same time interval lobe 3-2A also prograded northeastward into the Çandarlı Basin. Both lobes 2-2A and 3-2A reached their maximum extent at about 15 000 BP, immediately prior to the post glacial sea-level rise. Similarly, the Bakırçay delta (lobe 1-2B in Fig. 18) prograded westward into the Çandarlı Basin, where during the last phase of the delta advance the distal deltaic deposits of the Gediz and Bakırçay deltas coalesced (Fig. 18). Data from the northern portion of the Çandarlı Basin showed the progradation of a much smaller deltaic sediments, illustrated as lobe 1-2C in Figure 18. This small delta lobe is interpreted as the prograding foresets of the Madra river. In the northern Çandarlı Bay the distal sediments of this delta lobe also coalesce with those of the Gediz and Bakırçay deltas.

The outer Izmir Bay, in water depths of 70 to 110 m seaward of the Holocene Gediz and Bakırçay deltas, has a terrace-like surface morphology that varies in height from 4 to 20 ms (3 to 15 m @ 1500 m s^{-1}). The down-side of these terraces are almost always toward deeper water. In 3.5 kHz seismic profiles, they appear lenticular in shape and shingled one on top of the other in the landward direction. The uppermost reflectors of a particular lenticular unit onlaps a non-transparent zone on the landward side; and progrades over the underlying lenticular unit. The non-transparent zone is interpreted to represent the topset zone of the Pleistocene delta. The thickness of each lenticular unit varies between 15 and 30 ms (11.3 and 22.5 m) which, in the area, is the average penetration of the 3.5 kHz penetration. In the air-gun profiles the base of these lenticular units overlies the oblique prograding foresets of the depositional sequence 2. Their lengths are shortest (<1 km) immediately above the shelf break, becoming progressively longer landward (>5 km). Internally they exhibit weak to moderate, semi-continuous reflectors that run parallel to the lower surface of the unit. These lenticular units are interpreted as the coastal onlap deposits of the Holocene transgression.

Several inter-related factors controlled the dynamic equilibrium of the Gediz and bakırçay deltas from the last glacial maximum to present. During the peak of the last glacial period (ca. 20,000 yr BP) the sea-level was approximately 100 m lower than at present; it started to rise at around 16,000 yr BP with the maximum rise of about 50 m occurring between 12,000 and 8,000 yr BP (Clark *et al.* 1978). Observed fault throws show that the post-glacial sea-level rise around the western Turkey was accompanied by vertical crustal movements, including a subsidence of 1-2 m per 1000 years for the study area. These figures probably increased the actual water depth by 10 to 20 m during the last 10,000 years. The radiocarbon dates suggest that the progradation of the Pleistocene Gediz, Bakırçay and probably the Madra deltas ceased about 11,000 yr BP, but reworking of sands during the transgression continued until at least 7,000 yr BP.

All seismic lines examined from the outer Izmir Bay showed the topset zone of the Pleistocene Gediz delta devel-

oped around 150-180 ms (112.5-135 m) below present sea level. Whereas, this zone in the Pheistocene Gediz delta entering into the Çandarlı Basin is found to occur at about 160 ms (120 m) below present sea level. The topset zones of the Pleistocene Bakırçay and Madra deltas are developed around 140 ms (105 m) and 150 ms (112.5 m) below present sea level, respectively. These sediments were deposited under the repeated agitation of the water by waves and probably long shore currents. Around the present-day outer Izmir Bay and the Çandarlı Basin the average wave height and length are 0.5 m and 100 m respectively, with storm heights of about 2 m and length of 50 m. Sedimentological data in the area suggest that below about 20 m water depth the winnowing effect of the waves are minimal. Therefore, assuming that the prodelta shelf break during the last glacial maxima was at a water depth of about 20 m, the shoreline would have been situated at near the present day 95 m isobath. The stable isotopic data and the shallow-water, brackish benthic foraminiferal fauna found in cores recovered from water depths of 110-150 m suggest that the sea level was at least 100 m lower than at present, independently confirming the sea-level lowering suggested by the seismic data. Comparison of the various proposed sea-level curves showed that vertical uncertainties of 5-15 m, which for the topography of the area would translate into horizontal uncertainties of 1-1.5 km.

In the outer Izmir Bay, the depth of the shelf break (i.e. topset to foreset transition) progressively increases toward the north from about 110 m off Karaburun peninsula to more than 135 m immediately south of the island of Lesbos. No core data is available from the northernmost part of the shelf break, therefore no unequivocal dates can be given for the last phase of the delta advance. However, unless the northern outer Izmir Bay has preferentially subsided, the observed difference in the depth of the topset to foreset transition suggests that the Pleistocene Gediz river first abandoned the northern part of the lobe 2-2A (Fig. 18), perhaps as early as 14,000 yr BP during the early post-glacial transgression. This distributary abandonment during the early sea-level rise was compensated by high or balanced sediment influx so that there was a short stillstand of the delta distributary in the southern outer Izmir Bay. This area shows well-developed and thicker topset zone than the north, perhaps because delta sedimentation was concentrated in this area once effective regression of the shoreline began. Radiocarbon dates in cores recovered from the periphers of the Çandarlı basin penetrating into the topset deposits of the depositional sequence 2A and 2B showed that at about 14,000 yr BP the distributary of the Pleistocene Gediz delta (lobe 3-2A in Fig. 18) was abandoned, however, the distributary of the Bakırçay delta (lobe 1-2B in Fig. 18) remained active until about 10,000 yr BP. This is also supported by the occurrence of the topset to foreset transition in the western Çandarlı Bay at about 120 m, approximately 10 m below the same transition in the outer Izmir Bay.

The lenticular units of the coastal onlap deposits predominantly occur between 70 and 100 m isobaths. Published sea-level curves (Clark *et al.* 1978) suggest that approximately 25 m of sea level rise occurred between 16,000 and 11,000 yr BP, which assuming that the thickness of sediments accumulated during that time was compensated by tectonic subsidence, would put the 11,000 yr BP shoreline around the 70 m isobath. If the pre-transgression bottom topography of the area was similar to that of the present day, a metre rise in sea-level around the outer Izmir Bay wolud be translated into about 125 m of coastal retreat. From about 70 to 50 m isobaths, the slope of the outer bay is much gentler, so that a metre rise in the sea-level would produce about 750 m coastal retreat. During the rapid rise of sea-level from about 11,000 to 8,000 yr BP, delta progradation would be more difficult in the Izmir Bay, primarily because the sediments carried by the river would be dispersed over a much larger area. Thus, foreset progradation ceased and sediments were probably reworked and redistributed along the generally regressing coastline by waves and long shore currents, accounting for the lack of well-defined lenticular units landward of the 70 m isobath.

Published sea-level curves suggest that by around 6,000 yr BP the cost line would have retreated to approximately the 20 m isobath, except that part of the present Gediz and Bakır çay delta plains may also been flooded. According to the account of Plinius, Gediz river discharged near the city of Temnos some 3,000 yr BP. The delta prograded westward from about 3,000 to 2,000 yr BP forming the Maltepe and Mirmekes delta sub-lobes. From about 2,000 to 100 yr BP the delta progradation was mostly toward the southwest through the Değirmentepe, Kokala, Pelikan and Karşıyaka channels.

During a full cycle of high to low to high sea levels the Gediz and Bakırçay and probably the Madra deltas prograded approximately 40-65 km from the heads of bedrock-defined bays out to the shelf break and back to the heads again. Similar transgressive and regressive cycles would occur during every high to low to high cycle of sea level change. In our seismic profiles we recognise repeated cycles similar to this lateglacial to Holocene cycle. Periods of regression, stillstand, or slow transgression are marked by delta progradation. In our records, only the final phases of such progradation are visible near the modern shelf break, deposited shortly before rapid transgression terminated a depositional cycle.

Following the major transgression between isotopic stages 6 and 5e to a sea level stand above that of the present, delta fluctuations associated with the variations in sea level during isotopic stage 5 occurred within the ancestral Izmir Bay and are thus not recognised in our seismic profiles (because of multiples). During this sea-level high stand sapropels S3, S4 and S5 are deposited in the eastern Mediterranean. Only after continued deposition through stages 5 and 4, without any extreme marine high stands, did the deltas prograde to the outer shelf area. Continuing relatively low stands of sea level throughout stages 4, 3, and 2 mean that a fuller record of sea level fluctuation is preserved on the outer shelf during this time.

The Çandarlı Basin does not display such a long stratigraphic history as the outer Gediz delta. Our seismic profiles penetrate only to depositional sequence 3. The present day bathymetry of the region suggests that during the low stands of sea levels (-110 m; Aksu and Piper 1983), brackish or lacustrine conditions prevailed in Çandarlı Basin. The Bakırçay delta rapidly prograded westward in depositional sequences 3 and 2, largely filling a once larger Çandarlı Basin. Similarly the Madra delta prograded southward filling the northern portion of the Çandarlı Basin, at about the same time, a distributary of the Gediz delta temporarily occupied the western portion of Çandarlı Bay. This is clearly seen in Figure 8 where the distal deltaic deposits of the Gediz and Bakırçay river systems coalesce in Çandarlı Basin.

(2) Büyük Menderes and Küçük Menderes

Because we have good seismic coverage of Pleistocene delta formation only in the Küçük Menderes delta, we use this delta as an analogue for examining controls on wave dominated delta sedimentation. Depositional sequence 2 prograded during a gradual fall in sea level corresponding to isotopic stages 3 and 2. The overlying transgressive surface was formed during the Pleistocene to Holocene transgression (at the end of isotopic stage 2). Depositional sequence 1 accumulated during relatively stable sea-level conditios in the late

Holocene. The age of the lobes within depositional sequence 2 has been crudely estimated on the basis of their total volume and modern discharge rates of the river; this suggests that lobe 2C reached its maximum extent about 44 000 BP, lobe 2B at 30 000 BP and lobe 2A at 15 000 BP.

Lobe 2C prograded during the initial stages of the fall in sea level from the stage 3 high at about -40 m. The elevation of the distal part of lobe 2C indicates that it formed when sea level was at about -80 m. This lobe is estimated to have prograded from the headlands to its maximum extent in about 15,000 years. Progradation of the lobe terminated at the line joining Cape Sünger to Cape Karga (Fig. 23) which represents the next position seaward of the modern coastline at which the Küçük Menderes graben widens rapidly. The halting of delta advance at this position may, thus, represent a time when wave reworking was more important than fluvial processes. Lobe 2B prograded southwestward over lobe 2C, representing a return to fluvial dominance, perhaps as a result of more rap idly falling sea-level. Lobe 2B prograded for about 14,000 years reaching its maximum extent at around the present day 100 m isobath. At this time the distributary probably became over-extended, and eventually the Küçük Menderes river was diverted into a northwesterly course. Lobe 2A shows clear evidence or the progradation of a number of separate sub-lobes, similar to those observed in the Holocene Büyük Menderes delta. Progradation was terminated by the rapid post-glacial sea-level rise.

All seismic lines examined showed the topset to foreset transition in lobe 2A developed around 150-160 ms (112.5-120 m) below present sea level. It is dificult to precisely determine the amount of sea-level lowering from these data. The fault offsets in depositional sequence 3 suggest subsidence rates of 0.5-1 m per 1000 years, or 10-20 m since deposition of lobe 2A. The topset to foreset transition at the modern delta mouths occurs close to sea-level, but is at 10-20 m water depth on the wave cut platforms away from active mouths. The sandy Pleistocene topset sediments that were cored were deposited in a shallow coastal environment probably under the influence of waves, and thus, represent a depth range of a few metres to 20 m. Thus, the maximum Pleistocene sea-level lowering (some 20,000 yr BP) was about-110 m.

The very thin transgressive sediment sequence in the outer part of the Gulf of Kuşadası reflects the rapid sea-level rise from 16 000 to 8000 yr BP and implies that bottom topography of the Gulf of Kuşadası was similar to that of present day. During this early stage of the transgression foreset progradation did not take place, and sediments carried by the river were probably reworked and redistributed by waves and longshore currents. The ridge situated immediately landward of the shelf break (Fig. 7) probably represent a former barrier island system developed and drowned during this rapid transgression. As the sea level rose, the broad drowned delta platform damped the waves, so that more time would be required to build a barrier of the same size. Thus, the next evidence for prominent barrier island growth is seen after the rate of transgression had decreased. Barrier complexes are seen at the margin of the gulf, where they would be concentrated by littoral drift, in less than 70 m of water, and become widespread in the central part of the gulf only in water depths of less than 50 m.

Maximum transgression probably occurred around 6000 yr BP and the entire modern delta plains were flooded. Around 3000 yr BP, the shorelines in Küçük and Büyük Menderes deltas were situated east of Syrie Island and Dede Dağ, respectively (Figs. 3,4).

Archaeological and historical data suggest average delta progradation of 3 m a^{-1} over the last 3000 years for the Küçük Menderes rivers. Average delta progradation rates in depositional sequence 2 were less than 0.5 m a^{-1}. The large difference between the progradation rates during the last 3000 years and during the Late Pleistocene is due to both the geometry of the depocentre and its paleobathymetry, because the shelf area in which progradation took place during the late Pleistocene is much less constricted than the graben enclosing the modern delta plain. It is not clear whether the changes in the hinterland associated with climatic changes had increased or decreased the rate of erosion.

DISTRIBUTION OF FAULT-BOUNDED BASINS

(1) Gediz, Bakırçay and Madra

Many normal faults cut these complex deltaic sequences, and some are marked by surface breaks at the sea bed. In most faults, throws increase with subbottom depth, suggesting continual movement. Increased sediment accumulation on the downthrown side of some faults further suggests syn-

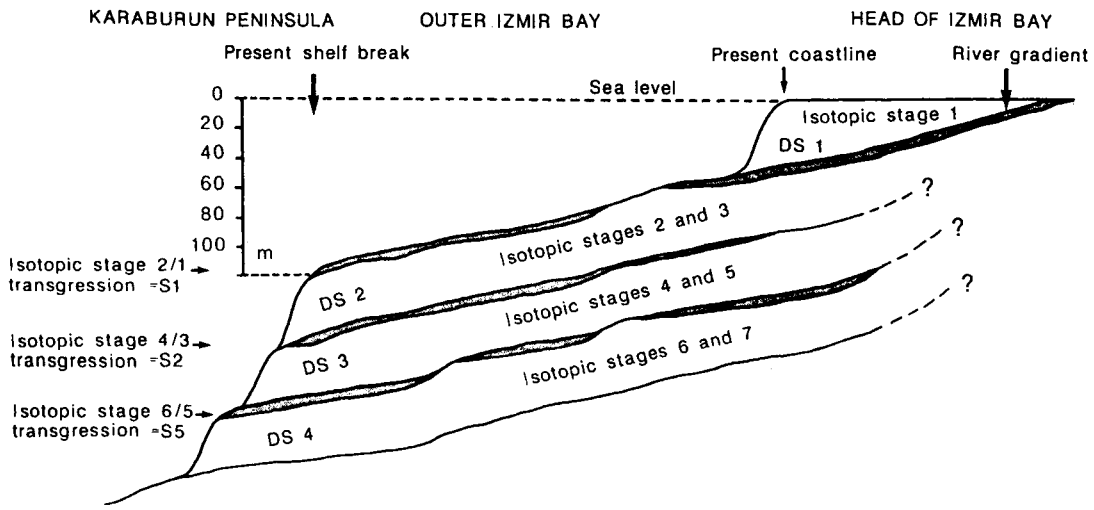

Fig. 28. Schematic illustration of depositional sequences as related to sea level changes in the Quaternary period.

Şekil 28. Kuvaterner dönemindeki deniz seviyesi değişimleriyle ilişkili depolanma istiflerinin şematik gösterimi.

depositional vertical movements. The relative offset of the 2/1 and 3/2 transgressive surfaces (Fig. 28) by these faults can be used to estimate the relative age of the two surfaces. In the Gediz and Bakırçay deltas, the offset of the 3/2 surface ranges from 3 to 6 times that of the 1/2 surface on any particular fault, with an average of 4.5 times. Assuming that the rate of movement on the faults is constant, this suggests that the 3/2 transgression surface is 4 or 5 times as old as the Holocene transgression surface.

Our grid of seismic lines is sufficiently dense to map the distribution of major faults in the Gediz and Bakırçay deltas. Figure 16 illustrates the most prominent faults that cut the reflector separating the depositional sequences 2 and 3. A series of NNW trending faults run approximately parallel to the present day coastline, forming the boundary of Izmir graben. Similarly, two major fault systems bound the eastern and western peripheries of the Çandarlı Basin. The southern extension of the major fault immediately east of the Karaburun peninsula can be correlated with the Karaburun-Ayvacik fault system. Kaya (1982) suggests that this fault system runs due north approximately parallelling the 26°38' N longitude, from the western Gülbahçe Bay to the eastern end of Lesbos Island (Fig. 29). The seismic data presented here show no evidence of a major fault system that crosses Izmir Bay, and suggest that the western boundary fault in the Çandarlı Basin may be correlated with the major Lesbos fault (Figs. 16,29).

The pre-Miocene tectonic framework (Fig. 29) is characterized by north-northeast trending fault blocks which have been interpreted as deep crustal fractures (Kaya 1981). These faults are cut orthogonally by a predominantly west-northwest running fault system. The latter fault system is the result of Late Miocene extensional tectonics and constitutes the earliest framework of the present day east-west aligned graben systems of western Anatolia (Kaya 1981). Comparison of the pre-Miocene and post-Miocene structural elements of the study area (Fig. 29) shows that only a limited number of pre-Miocene faults were active during the Quaternary period. The fault data discussed here indicate that in Izmir Bay and Çandarlı Basin, the Quaternary tectonic subsidence took place along a reactivated pre-Miocene structural fabric. The data also suggest that the subsidence may be strongly influenced by the loading effect of the advancing deltas during the low stands of sea levels.

(2) Büyük Menderes and Küçük Menderes

High angle-normal faults also cut the depositional sequences 2 to 4 in the Küçük Menderes delta (Fig. 7). In a few places faults also cut depositional sequence 1, forming distinct steps at the sea floor. The frequent seismic profile crossovers allow correlation of faults over the Gulf of Kuşadası. The most prominent faults that cut the reflector separating depositional sequences 2 and 3 are mapped in Figure 22. The tectonic framework of the Gulf is characterized by a network of roughly E-W trending faults. North of 37°55' N latitude all major faults have their downthrown sides to the south, whereas in the southern part of the Gulf faults are downthrown to the north. These faults thus, form a major E-W graben system in the centre of the Gulf of Kuşadası (Fig. 22). Fault throws in depositional sequence 3 of about 150 ms (112.5 m) are observed in the central Gulf, whereas throws are less than 50 ms (37.5 m) in the northern and southern Gulf.

DEFORMATIONAL STRUCTURES

Several structures related to post-sedimentary deformation are identified in the seismic profiles, including peripheral slumping, deep-seated flowage and soft sediment deformation related to faulting. Peripheral slumping is identified in the 3.5-kHz profiles where displacement of coherent masses, with little or no internal deformation, rotated downslope along discrete shear planes. This is best observed in sediments immediately seaward of the topset to foreset transition of the deltas. Rotational slumping was probably triggered by seismic activity and occurred where slopes were oversteepened by rapid

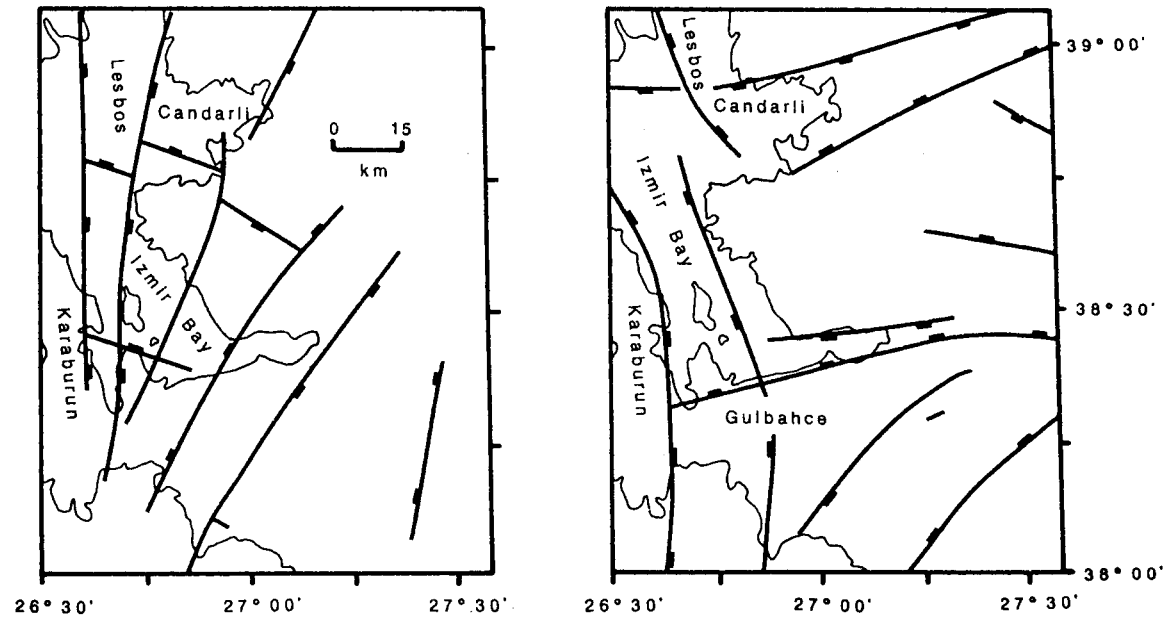

Fig. 29. Pre-Miocene (left) and post-Miocene (right) structural elements of Izmir and Çandarlı bays, data from Kaya (1981) and Dewey yand Şengör (1979) respectively. Major Quaternary fault patterns are also shown.

Şekil 29. İzmir ve Çandarlı körfezinin Miyosen öncesi (Kaya, 1981) (sol) ve Miyosen sonrası (Dewey, Şengör, 1979) (sağ) yapısal elementleri, Kuvaterner dönemine ait belirgin faylanmalar da dahil edilmiştir.

deposition of river mouth sediments.

Deep-seated flowage is commonly observed in seismic profiles running adjacent to major faults. The distal end of depositional sequence 3 in the outer Izmir Bay, immediately below the present day shelf break, exhibits a seismic package with internally undulating reflectors that run nearly parallel to each other (Fig. 30). Occasional diapiric folds also occur within this package as isolated blocks. The inflection of the sea floor, as well as at the base of depositional sequence 2 landward of the shelf break, suggests that considerable subsidence took place in this area. These deformational features are seen only in line I-I' (Fig. 30), which runs parallel to the Karaburun-Ayvacik fault (Fig. 16); a seismic line less than 10 km northeast (G-G') shows no evidence of deep-seated flowage (Figs. 15,30). Comparison of sediment thickness between lines I-I' and G-G' shows that in the deformed section depositional sequence 3 is about 30 msec (24 m @ 1600/sec two-way time) thinner. The seismic character of depositional sequence 3 suggests that the deformation took place during the last phase of delta progradation of depositional sequence 2, possibly due to loading effects coupled with movement along the Karaburun-Ayvacik fault. Similar deformation is also seen in depositional sequence 4 (Fig. 30). Figure 30 also shows several fault related soft sediment deformations.

DISCUSSION

All four deltas discussed occupy the heads of major east-west grabens that extend from the continent to the adjacent continental shelf and back-arc basin. Although the sea level has fluctuated by over 100 m during their late Quaternary growth, even at low stands of sea level, the deltas would have formed at the head of an elongate marine bay within a graben (Fig. 1), where the 100 m contour approximates the Late Pleistocene shoreline.

Fluvial and deltaic graben sediments are major components of the thick post-orogenic sediment sequences that accumulate in many successor basins. These deltas thus, occupy a tectonic setting that is common in the geological record, for example in the Carboniferous strata of Europe and eastern Canada. The fluctuations in sea level during the Pleistocene provide a natural laboratory to understand how sea-level changes (whether eustatic or epirogenic) affect delta architecture and sediment facies. Similar fluctuations in sea level probably affected delta growth at earlier times of major glaciations, such as the Late Ordovician and the Permo-Carboniferous.

Despite their apparent sheltered settings within grabens, the morphology of the present-day Büyük Menderes and Küçük Menderes deltas and the Pleistocene Gediz and probably Bakırçay deltas indicates that they are high destructive, wave dominated deltas. In the microtidal setting of the Mediterranean, wave process predominate over tidal processes. Offshore gradient and fetch are sufficient to permit significant wave activity, despite the presence of offshore islands (horsts) which limit the effectiveness of deep water waves. The regional channel gradients are maintained by tectonic subsidence, so that at times of falling sea level, braided river courses may extend over much of the delta plain. Very steep foresets close to river mouths represent delivery of sand to the prodelta slope. Much of the delta progradation takes place by deposition of mud on the prodelta slope; this process predominates at times of delta progradation with a stable sea level, when meandering channels and extensive delta plains trap much of the coarse sediments upstream. Both archaeological data (Figs. 2, 3, 4) and seismic analysis (Figs. 18, 23) show that even within a narrow graben the delta progrades through lobe growth, first on one side of the graben, then on the other side.

Places where the graben widens rapidly, such as at the present coastline of the Küçük Menderes, are sites of maximum wave activity. As a result, during successive transgressions and regressions, delta progradation will tend to pause at such points, leading to the development of thick barrier sand complexes as delta mouth sediments are reworked. Such sites, which are tectonically controlled, may thus preferentially develop sand facies during basin subsidence.

Rapid transgressions are a feature of the Quaternary as a result of rapid retreat of terrestrial ice-sheets. They result in rapid retreat of the delta shoreline over distances of many tens of kilometres. There is no evidence for delta mouth progradation during these transgressions, which produce a thin transgressive sand sheet over the surface of the delta. Because progradation is inhibited during the rapid transgression, initial deposition following the stabilization of sea level takes place in a highly sheltered environment, and the delta builds into relatively shallow water, so that progradation is rapid. Both the sheltered position and rapid progradation inhibit the development of sandy beach ridges.

CONCLUSIONS

Seismic reflection profiling and geological studies have shown that delta architecture in rapidly subsiding basins in western Turkey is largely controlled by glacially induced changes in sea level. Major interglacials of tens of thousands of years duration (such as in isotopic stages 1 and 5) are marked by major transgressions during which thin lenticular coastal deposits accumulate as the shoreline retreats. At the maximum extent of the sea, the transgression extended up shallow alluvial valleys in which islands and bedrock promontories protect the coast from direct wave attack. The subsequent initial progradation phase is rapid in the shallow sheltered waters. In the case of the Holocene transgression this progradation phase occurred in classical times, ending about 100 AD as the coastline reached a position exposed to southwesterly winds. In the Gediz delta, Izmir Bay is larger and deeper and has not yet been completely filled.

Holocene Büyük Menderes illustrates the style of progradation of a wave-dominated delta entering deeper water. Successive delta lobes build out as the river mouth shifts, and abandoned lobes are subjected to erosion. Barrier beaches develop as abandoned river mouth sands are re-dispersed. The transition from topset to foreset strata occurs in water depths of a few to ten metres. Holocene Gediz, however, illustrates the style of progradation of a river-dominated delta entering deeper water. There are at least six shifts in the position of the Gediz mouth during the last ca. 3,000 years and abandoned delta-top channels can be correlated with submarine delta lobe sequences.

The continental shelf and slope in the grabens of western Turkey developed as a result of similar delta progradation during Pleistocene glacial periods when sea level was generally tens of metres below that of interglacials. Fluctuations in sea level are recorded in changes in the elevation of topset to foreset transitions, but no major transgressions are recognized except during full interglacials.

The continental shelf around the Aegean Sea shows considerable variations in width (Fig. 31). It varies from less than 5 km along the east and west Peleponnese, east of Evvoia Island and off southwest Anatolia to 40-60 km along the northern Aegean Sea and western Anatolia. The depth of the shelf break is around 110-170 m and gentle slopes lead to depths of 300-500 m. At these depths a second break in the slope gradient occurs and steeper slopes lead to throughs

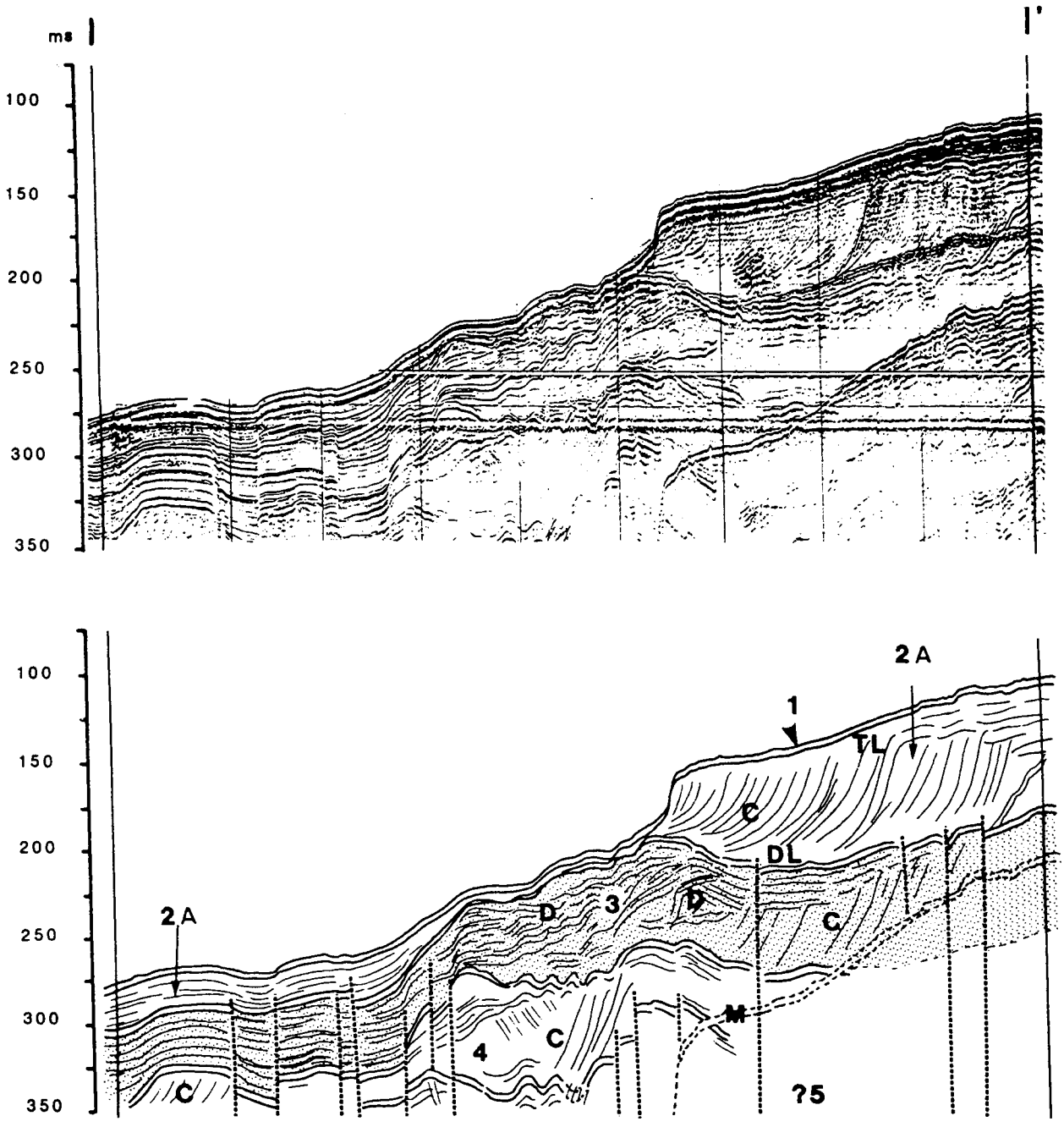

Fig. 30. Air-gun seismic profile (I-I') across the shelf break off Izmir Bay. Location is shown in Figure 2. 1 to 4 are depositional sequences; 2A is the depositional sequence related to the progradation of Gediz delta. TL= toplap, DL= downlap, C= clinoforms, M= multiple, D= sediment deformation, dashed lines= faults. Profile is about 14 km long, vertical exaggeration= 37.

Şekil 30. İzmir Körfezi açıklarından alınmış hava tabancası sismik profili (I-I'). Kesit konumu Şekil 2'de verilmiştir. 1-4 depolanma istifleri olup, 2A Gediz Deltasının ilerleyişi ile ilgili depolanma istifidir. TL= toplap, DL= downlap, C= klinoformlar, M= tekrarlı yansımalar, D= sediment deformasyonu, kesikli çizgiler= faylar. Profil uzunluğu 14 km olup, düşey abartma ise 37'dir.

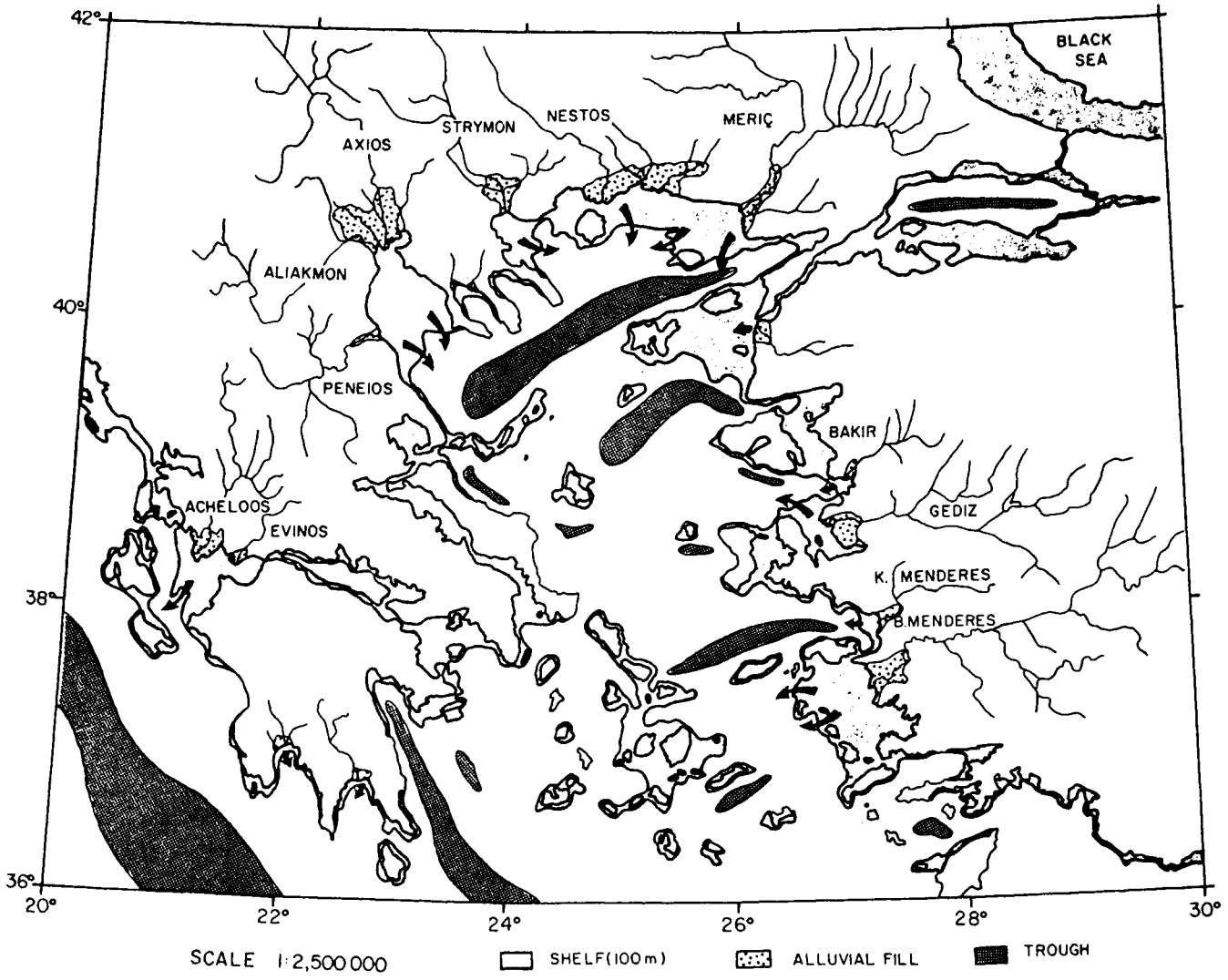

Fig. 31. Map of the Aegean Sea and adjacent regions showing coastal areas of subaerial alluvium, continental shelves resulting from delta progradation, and deeper troughs accumulating turbidites.

Şekil 31. Ege Denizi ve çevresinde kıyısal alüvyon birikim alanları, delta ilerlemesiyle oluşan kıta sahanlığı ve türbidit birikimlerinin olduğu derin havzalar.

where water depth exceeds 1500 m. The widest shelves occur off the mouths of major rivers, suggesting that the growth pattern observed in the deltas discussed in this paper may be general. It is suggested that similar delta progradation has occurred off most major rivers during maximum low stands of the sea-levels. The sediment distribution pattern and the relationship between major depositional features and sea-floor morphology studied in the eastern Aegean Sea may thus serve as a model for many areas of the eastern Mediterranean Sea.

SUMMARY

(1) The shelf area of the eastern Aegean Sea off major rivers is formed of superimposed deltaic sequences. Deltas prograded seaward during low stands of sea level. The present day shelf break denotes the topset to foreset transition of progradation during the last glacial period. The relative position of the shelf break during earlier interglacial periods varied depending on the maximum lowering of sea level and the subsidence rates.

(2) Following post glacial transgressions deltas were reestablished deep in ancestral bays and little sedimentation took place on the shelf area during the interglacial periods.

(3) In Gulf of Kuşadası, the outer Izmir Bay and Çandarlı Basin the Quaternary tectonic subsidence was about 1 m per 1000 years and took place along the reactivated pre-Miocene structural fabric. The primary cause of this subsidence is probably the continued N-S extension of the Aegean plate but it is also affected by the loading effect of the stacked deltas.

(4) Penecontemporaneous and post sedimentary deformations are common and widespread in the Quuaternary deltaic sequences. This type of deformation may be far common in ancient deltaic sequences than generally recognized.

ACKNOWLEDGEMENTS

The authors owe special thanks to Prof. Dr. Erol Izdar, the Director of the Institute of Marine Sciences and Technology; without his continued support and encouragement it would have been impossible to carry out this research. Travel funds from NATO and Dalhousie University to Aksu and Piper, and research funds from NSERC to Aksu and Piper were acknowledged. Special thanks are due to the crew and scientific personnel of the research vessel "Koca Piri Reis" of the 79-IZ, 84-IZ and 85-IZ cruises. Phil Hill of the Bedford Institute of Oceanograaphy and Richard Hyde of the Department of Earth Sciences, Memorial University of Newfoundland critically read the manuscript. Text figures are drafted by Larry Nolan.

REFERENCES

Aksu, A.E. 1981. Late Quaternary Stratigraphy, Paleoenvironment and Sedimentation History of Baffin Bay and Davis Strait. PhD Thesis, Dalhousie University, Halifax, NS, Canada, 771p.

Aksu, A.E. and Piper, D.J.W. 1983, Progradation of the late Quaternary Gediz delta, Turkey. Mar. Geol. 54, 1-25.

Aksu, A.E. 1985. Planktonic foraminiferal and oxygen isotopic stratigraphy of CESAR cores 102 and 103: preliminary results. *In*: Initial Geological Report on CESAR - the Canadian Expedition to Study the Alpha Ridge, Arctic Ocean. Geological Survey of Canada, Paper 84-22, 115-124.

Aksu, A.E., Piper, D.J.W. and Konuk, T. 1987a, Late Quaternary tectonic and sedimentation history of outer Izmir and Çandarlı Bays, western Turkey. Mar. Geol. 76,89-104.

Aksu, A.E., Piper, D.J.W. , and Konuk, T., 1987b. Quaternary growth patterns of Büyük Menderes and Küçük Menderes deltas, western Turkey. Sediment. Geol. 52, 227-250.

Angelier, J., Dumont, J.K., Karamanderesi, H., Poisson, P., Şimşek, S. and Uysal, S. 1981, Analysis of fault mechanisms and expansion of southwestern Anatolia since the late Miocene. Tectonophysics 75, T1 - T9.

Arpat, E. and Şaroğlu, F. 1975, Türkiye'deki bazı genç tektonik olaylar. Bull. Geol. Soc. Turkey 18, 91 - 101.

Bean, G.E., 1966. Aegean Turkey - An Archaeological Guide. Benn London, 288 p.

Cita, M.B., Vergnaud-Grazzini, C., Robert, D., Chamley, H., Ciaranfi, N. and D'Onofrio, S. 1977, Paleoclimatic record of a long deep-sea core from the eastren Mediterranean. Quat. Res. 8, 205-235.

Clark, J.A., Farrell, W.E. and Peltier, W.R. 1978, Global changes in post-glacial sea level: a numerical calculation. Quat. Res. 9, 265-287.

Dewey, F.J. and Şengör, A.M.C. 1979, Aegean and surrounding regions: complex multiplate and continuum tectonics in a convergent zone. Geol. Soc. Am. Bull. 90, 84-92.

EIEI 1981, Elektrik İşleri Etüd İdaresi, 1981 su yılı akım neticeleri.

Eisma, D. 1978, Stream deposition and erosion by the eastern shore of the Aegean. In: W.C. Brice (Editor), the Environmental History of the Near and Middle East Since the Last Ice Age. Academic Press, London, 67-81.

Erinç, S. 1955, Gediz ve Küçük Menderes deltalarının morfolojisi. (The Morphology of Gediz and Küçük Menderes deltas). IX Coğrafya Meslek Haftası Tebliğler ve Konferanslar, Türkiye Coğrafya Kurumu 1, 33-66.

Erinç, S. 1978, Changes in the physical environment in Turkey since the end of last glacial. In: W.CC. Brice (Editor), The Environmental History of the Near and Middle East Since the Last Ice Age. Academic Press, London, 87-110.

Flemming, N.C. 1972, Eustatic and tectonic factors in the relative displacement of the Aegean coast. In: D.J. Stanley (Editor), The Mediterranean sea: A Natural Sedimentation Laboratory. Dowden, Hutchinson and Ross Inc., Stroudsburg, 189-201.

Galanopoulos, A. and Delibasis, N. 1971, Seismotectonic map of Greece. The Seismological Institute of the National Observatory of Athens and the Institute for Geology and Subsurface Research of Greece. Published by: The Institute for Geology and Subsurface Research, Athens, Greece., 1:100,000 scale.

Kaya, O. 1981, Miocene reference section for the coastal parts of west Anatolia. Newsl. Stratigr. 10(3), 164-191.

Kaya, O. 1982, Tersiyer sırt yitmesi: Doğu Ege bölgelerinin yapısı ve magmatiği için olasalı bir mekanizma (A possible mechanism for the structure and magmatism of the eastern Aegean region). In: O. Erol and V. Oygur (Editors), Batı Anadolu'nun Genç Tektoniği ve Volkanizması. Türkiye Jeoloji Kurultayı Paneli, Ankara, 39-58.

Lykousis, V., Collins, M.B. and Ferentinos, G. 1981, Modern Sedimentation in the NW Aegean Sea. Mar. Geol. 43, 111-130.

Mitchum, R.A.Jr., Vail, P.R. and Thompson III, S. 1977, Seismic stratigraaphy and global change of sea level. Part 2: The depositional sequence as a basic unit for stratigraphic analysis. In: C.E. Payton (Editor), Seismic Stratigraphy Applications to Hydrocarbon Exploration. Am. Assoc. Pet. Geol. Mem. 25, 53-62.

Piper, D.J.W. and Panagos, A.G. 1981, Growth patterns of the Acheloos and Evinos deltas, western Greece. Sediment. Geol., 28, 111-132.

Russell, R.J. 1954, Alluvial morphology of Anatolian Rivers. Ann. Assoc. Am. Geogr., 44, 363 - 391.

Saatçi, F. and Taysun, A. 1979, Kemalpaşa, Turgutlu ve Salihli civarındaki bazı yan derelerin farklı zamanlardaki iyon ve sediment konsantrasyonlarının değişimi üzerine araştırmalar. (The ion and sediment concentrations of some small rivers near Kemalpaşa, Turgutlu and Salihli). Ege University, Faculty of Agriculture Bulletin 16, 17-40.

Shackleton, N.J. and Opdyke, N.D. 1976, Oxygen isotope and paleomagnetic stratigraphy of Pacific core V28-239 Late Pliocene to latest Pleistocene. In: R.M. Cline and J.D. Hays (Editors), Investigation of Late Quaternary Paleoceanograhpy and paleoclimatology. Geol. Soc. Am. Mem. 145, 449-464.

Stanley, D.J. and Blanpied, C. 1980, Late Quaternary water exchange between the eastern Mediterranean and Black Sea. Nature 285, 537-541.

Stearns, C.e. and Thurber, D.L. 1965, Th-230 and U,234 dates of Late Pleistocene marine fossils from the Mediterranean and Moroccan littorals. Quaternaria 7, 29-42.

Thunell, R.C., Williams, D.F. and Kennett, J.P. 1977, Late Quaternary paleoclimatolgy, stratigraphy and sapropel history in eastern Mediterranean deep-sea sediments. Mar. Micropaleontol. 2, 271-388.

Thunell, R.C. 1978, Distribution of recent planktonic foraminifera in surface sediments of the Mediterranean Sea. Mar. Micropaleontol. 3, 147-173.

Topraksu 1980, Topraksu İstatistik Bülteni No: 305. Topraksu Genel Müdürlüğü Yayını, Ankara, Turkey.

Unesco 1969. Discharge of Selective Rivers of the World. Studies and Reports in Hydrology 1, 70p.

Venkatarathnam, K., Biscay, P.E. and Ryan, W.B.F. 1972, Origin and dispersal of Holocene sediments in the eastern Mediterranean Sea. In: D.J. Stanley (Editor), The Mediterranean Sea: A Natural Sedimentation Laboratory. Dowden, Hutchinson and Ross Inc., Stroudsburg, 455-469.

Vergnaud-Grazzini, Ryan, W.B.F. and Cita, M.B. 1977, Stable isotopic fractination, climate change and episodic stagnation in the eastern Mediterranean during the Late Quaternary. Mar. Micropaleontol. 2, 353-370